SHORT COMMUNICATION

Endogenous ZAP is associated with altered global cellular gene expression during Zika virus infection

Nguyen Phuong Khanh Le[1], Prince Pal Singh[1,2], Ivan Trus[3], Uladzimir Karniychuk[1,*]

[1]Department of Veterinary Biosciences, College of Veterinary Medicine, The Ohio State University, Columbus, OH, USA

[2]School of Public Health, University of Saskatchewan, Saskatoon, Canada

[3]Dioscuri Centre for RNA-Protein Interactions in Human Health and Disease, International Institute of Molecular and Cell Biology, Warsaw, Poland

*** Correspondence:** Uladzimir Karniychuk

Department of Veterinary Biosciences, College of Veterinary Medicine, The Ohio State University, Columbus, OH, USA

karniychuk.1@osu.edu

Abstract

The zinc finger antiviral protein 1 (ZAP) has broad antiviral activity. Previous RNA-seq analyses were conducted in uninfected wild-type and ZAP-KO cells; however, the impact of ZAP on global gene expression during virus infection remains unknown. Here, we characterized global cellular gene expression in uninfected and Zika virus-infected wild-type and ZAP knockout VERO cells. ZAP is an interferon (IFN)-stimulated gene, which itself may enhance type I IFN antiviral response. We found that ZAP was associated with the inhibition of Zika virus in the absence of a robust type I IFN system (VERO cells are deficient for IFN-alpha and -beta). Also, during Zika infection in VERO cells endogenous ZAP was associated with amplification of global transcriptional antiviral responses in the absence of a robust type I IFN system. Further studies are warranted to elucidate this type I IFN-independent antiviral activity directly or indirectly mediated by ZAP.

Keywords: **Flavivirus, Zika virus, Zinc finger antiviral protein, ZAP, interferon, RNA-seq**

44 **INTRODUCTION**

45 The zinc finger CCCH-type antiviral protein 1 (ZAP) is a cellular protein with broad antiviral
46 activity [1-5]. ZAP binds viral RNA mediating degradation and translational inhibition [3].
47 While ZAP lacks intrinsic RNase activity, it recruits the 5′ and 3′ RNA degradation machinery
48 [6,7]. Using a murine leukemia reporter virus, DDX17 and DHX30 cellular RNA helicases were
49 identified as ZAP co-factors [8,9]. The E3 ubiquitin ligase TRIM25 enhances ZAP activity
50 against alphaviruses [10,11]. ZAP also interacts with the cytoplasmic protein KHNYN to inhibit
51 CpG-enriched human immunodeficiency virus 1 (HIV-1) [12]. Recently, Riplet, a protein known
52 for activating the retinoic acid-inducible gene I, was identified as a ZAP co-factor [13]. Initially
53 characterized to inhibit murine leukemia virus [14], ZAP has shown efficacy against many
54 viruses, including alphaviruses, filoviruses, influenza virus, porcine reproductive and respiratory
55 syndrome virus , hepatitis B virus, human cytomegalovirus, human T-cell lymphotropic virus
56 type 1, and HIV-1 [1,15-24]. However, ZAP's antiviral efficiency is limited against certain RNA
57 viruses, including vesicular stomatitis virus, poliovirus, enterovirus A71, herpes simplex virus
58 type 1, and some flaviviruses [7,15,25]. Emerging flaviviruses constantly threaten public health.
59 A previous study showed the sensitivity of Japanese encephalitis virus (JEV) to overexpressed
60 ectopic and endogenous ZAP [7]. In contrast, yellow fever virus (YFV), dengue virus (DENV),
61 and Zika virus were categorized as ZAP-resistant [7,15]. Zika virus sensitivity was tested by
62 ectopically overexpressing ZAP against the background of endogenous ZAP. Overexpression
63 screening is a powerful approach, but overexpressing individual genes may also miss antiviral
64 effectors that work in multiprotein complexes [26]. Here, we compared Zika virus RNA loads
65 and characterized global cellular gene expression in uninfected and Zika-infected wild-type and
66 ZAP knockout VERO cells.

67 **MATERIALS AND METHODS**

68 **Cells**

69 We maintained wild-type VERO E6 cells (ATCC; VERO-ZAP-WT) and ZAP knockout (ZAP-
70 KO) derivatives (VERO-ZAP-KO) in DMEM supplemented with 10% heat-inactivated fetal
71 bovine serum (FBS), 1x Penicillin-Streptomycin, and 2.67 mM sodium bicarbonate at +37°C in a
72 5% CO_2 humidified incubator. To generate ZAP-KO cell line, we used the guide RNA (gRNA)
73 GTCTCTGGCAGTACTTGCGA which targets the first exon of *Chlorocebus sabaeus* (Gene ID:
74 103226990) ZC3HAV1 gene, which is required for the expression of all ZAP isoforms. We also
75 used a non-targeting control gRNA ACGGAGGCTAAGCGTCGCAA. These gRNAs were
76 transiently transfected into cells using GenCrispr NLS-Cas9-NLS Nuclease (GenScript).
77 Subsequently, transfected cells were seeded in 96-well plates through limiting dilution to
78 generate isogenic single clones. Following expansion, the clones were genotyped via Sanger
79 sequencing, employing primers (ATCGCTGGGCTGGACTAACG,
80 GCAGAGAAGGGAGTGGCTGAA) to identify indels. The knockout subclone verified by
81 genotyping was further confirmed by western blot for ZAP expression (**Fig 1A**) as described
82 below. We confirmed the absence of mycoplasma contamination in cells using the LookOut
83 Mycoplasma PCR Detection Kit (Millipore Sigma).

84

85 **Western blot**

86 Cells cultured in T-175 flasks were washed, pelletized, and lysed in 300 µL of RIPA buffer
87 (Fisher) supplemented with 1× Halt protease inhibitor cocktail (Fisher) and 1× EDTA (Fisher).
88 The lysates were then incubated on wet ice for 10 minutes, gently vortexed, and centrifuged
89 (12,000g, 10 min, +4 °C). Supernatants were aliquoted into prechilled low protein binding tubes

90 (Sarstedt) and stored at -80°C. After quantifying protein concentration with the Pierce BCA
91 Protein Assay Kit (Fisher), 50 µg of protein extract was diluted in 4× reducing Laemmli SDS
92 sample buffer (Fisher), heated at 95ºC for 10 min, and resolved on 10% Mini-PROTEAN TGX
93 precast protein gels (Bio-Rad) in 1× Tris/Glycine/SDS running buffer (Bio-Rad) at a voltage of
94 125V for 70 min. Proteins were transferred on methanol-activated 0.45 µm Immun-Blot Low
95 Fluorescence polyvinylidene fluoride (PVDF) membranes using the Trans-Blot Turbo RTA Mini
96 0.45 µm LF PVDF Transfer Kit (Bio-Rad, Cat. 1704274). The PVDF membranes were blocked
97 with 1× VWR Life Science Rapidblock Blocking Solution (VWR) for 1 h at room temperature.
98 Subsequently, the membranes were incubated overnight at +4°C with primary antibody diluted in
99 blocking solution. The membranes were washed four times with TBST (1× Bio-Rad Tris
100 Buffered Saline containing 0.1% Tween-20) and then incubated with secondary antibody, along
101 with hFAB Rhodamine Anti-Actin Primary Antibody (Recombinant human β-actin), diluted in
102 Blocking Solution for 1 h at room temperature, and washed four times with TBST. Fluorescent
103 blots were imaged on the ChemiDoc MP Imaging system using an appropriate detection channel
104 with Image Lab Touch Software (Bio-Rad).
105 We used antibodies (Abs): Rabbit anti-ZAP IgG Abs (1:1,000 dilution; ANTI-ZC3HAV1
106 HPA059096-100UL, Sigma-Aldrich), hFAB Rhodamine Anti-Actin Primary Abs (1:2,500;
107 #12004164, BIO-RAD), and IRDye 680RD Goat anti-Rabbit IgG secondary Abs (1:10,000; 926-
108 68071, LI-COR).
109
110 **Viruses**
111 We utilized the Asian lineage Zika virus H/PF/2013 strain [GenBank: KJ776791.2]. Zika virus
112 was synthetically rescued using reverse genetics following previously described methods [27].

113 Subsequently, the virus was propagated in VERO cells cultured in DMEM supplemented with
114 2% FBS and 1% penicillin/streptomycin (P/S). Supernatants were harvested, centrifuged (12,000
115 g, 20 min, +4°C), aliquoted, and frozen (-80°C). Infectious virus titers were quantified using
116 VERO cells via the endpoint dilution assay. The fifty percent tissue culture infective dose
117 ($TCID_{50}$) endpoint titers were calculated as previously described [27-30]. Media from virus-
118 negative VERO cells was processed in the same manner as the virus stocks and used as control.
119 The absence of mycoplasma contamination in the virus stocks was confirmed using the LookOut
120 Mycoplasma PCR Detection Kit (Millipore Sigma).
121

122 **Comparative RNA-seq analysis in wild-type and ZAP-KO cells**

123 VERO-ZAP-WT and VERO-ZAP-KO cells were seeded at 6×10^5 cells per well in 6-well plates,
124 with 4 plates per cell line, in DMEM supplemented with 10% FBS for 24 h. Wells in two plates
125 from each cell line were either mock-inoculated with media from virus-negative cells (4-6 well
126 replicates for VERO-ZAP-WT and VERO-ZAP-KO) or inoculated with a multiplicity of
127 injection (MOI) of 1 of Zika virus (6 well replicates for VERO-ZAP-WT and VERO-ZAP-KO).
128 After 2 h at 37ºC, the inoculum was removed, cells were washed, and covered with DMEM
129 supplemented with 2% FBS, then maintained at 37ºC. At 24 and 72 h post-inoculation, media
130 was removed, cells were washed with commercial 1× PBS, homogenized in 1 mL of TRI
131 Reagent Solution (Fisher), and RNA was extracted according to the manufacturer's protocol
132 using the PureLink RNA Mini Kit (Fisher). A total of 4-6 replicate samples were obtained for
133 mock-inoculated VERO-ZAP-WT, mock-inoculated VERO-ZAP-KO, Zika-infected VERO-
134 ZAP-WT, and Zika-infected VERO-ZAP-KO cells, at both 24 and 72 h.

135 RNA quantification was performed using the Qubit high sensitivity assay kit (Invitrogen) and
136 Qubit 2.0 Fluorometer (Invitrogen). RNA quality was assessed using a bioanalyzer (Agilent
137 Technologies 2100) to ensure all samples had RNA Integrity Number (RIN) values above 9.0.
138 DNA contamination was removed using the TURBO DNA-free Kit (Fisher). mRNA with intact
139 poly(A) tails was enriched using the NEBNext Poly(A) mRNA Magnetic Isolation Module
140 (NEB) and utilized for library constructions with the NEBNext Ultra II Directional RNA Library
141 Prep Kit for Illumina along with NEBNext Multiplex Oligos for Illumina (96 Unique Dual Index
142 Primer Pairs; NEB). The libraries were sequenced on the NovaSeq platform as paired-end reads
143 using the S1 v1.5 kit with 300 cycles (Illumina). FASTQ files were trimmed for adaptor
144 sequences and filtered for low-quality reads using *Trimmomatic*. RNA-seq analysis was
145 conducted as previously described [30-33] with modifications. Briefly, paired-end reads were
146 processed using the *Kallisto* pseudo-alignment method [34] and quantified by mapping to a
147 transcripts database generated from the African Green Monkey (vervet) reference genome
148 assembly (ENSEMBL *Chlorocebus sabaeus* 1.1) [35]. The count table for RNA-seq data was
149 assembled using the *tximport::tximport* function in R. After importing data to the R environment
150 we removed data for genes with low expression using the *edgeR::filterByExpr* function [36].
151 Normalization was then performed using the *edgeR::calcNormFactors* function, and the
152 *limma::voom* function was used to convert the data into a normal distribution. We calculated
153 differential expression using the *limma::lmFit* function with empirical Bayes moderation via the
154 *limma::eBayes* function (**Table S1**). Finally, we performed a gene set enrichment analysis using
155 the *limma::camera* function. Gene set enrichment analysis was conducted using Gene Ontology
156 (GO) annotation for *Chlorocebus sabaeus* obtained from g:Profiler [37]. Raw data were
157 deposited to NCBI BioProject (PRJNA1101086).

158 The following analytical strategy was chosen to normalize for intrinsic transcriptional
159 differences (**Tables S2A-D**) and compare RNA-seq data between Zika virus-infected ZAP-WT
160 cells and Zika virus-infected ZAP-KO cells. Initially, we compared transcriptional responses
161 between non-infected and infected VERO-ZAP-WT cells. Subsequently, we compared
162 transcriptional responses between non-infected and infected VERO-ZAP-KO cells. Finally,
163 affected genes and GO processes were summarized in **Table S2** and figures, and pairwise
164 comparison of genes and comparative GO analysis between VERO-ZAP-WT and VERO-ZAP-
165 KO cells were conducted (**Figs 2-4**; **Fig S1; Table S2**).
166

167 **Reverse transcriptase quantitative polymerase chain reaction assays (RT-qPCR)**

168 The portion of RNA from all RNA-seq samples described above was used to quantify
169 intracellular Zika virus RNA with a virus-specific RT-qPCR assay. All RT-qPCR reactions were
170 performed on the QuantStudio 3 real-time PCR system (Applied Biosystems) and analyzed using
171 QuantStudio Design & Analysis Software v1.5.2.
172 For Zika virus RNA quantification, a previously validated SYBR one-step RT-qPCR assay was
173 used [42]. The reaction mixture (20 µL) of the Luna Universal One-Step RT-qPCR Kit (NEB)
174 comprised 10 µL Luna Universal One-Step Reaction Mix, 1 µL Luna WarmStart RT Enzyme
175 Mix, 0.8 µL (10 µM) each of forward (ZIKV-F-SYBR: 5′-
176 AGGATCATAGGTGATGAAGAAAAGT-3′) and reverse (ZIKV-R-SYBR: 5′-
177 CCTGACAACACTAAGATTGGTGC-3′) primers, 3.4 µL nuclease-free water, and 4 µL of
178 RNA template. The reverse transcription and enzyme activation steps of 10 min at 55°C and 1
179 min at 95°C were followed by 40 amplification cycles (10 s at 95°C and 60 s at 60°C). For a
180 standard curve, we generated complementary DNA fragment using viral RNA as a template and

181 primers (T7-F3- TAATACGACTCACTATAGGGCACCACCTGGGCTG; R3-
182 ACAGGCTGCACAGCTTTCCC) containing the T7 promoter. Afterward, the DNA template
183 was transcribed with the MAXIscript™ T7 Transcription Kit (Invitrogen) to generate Zika virus
184 RNA. DNA was removed with the TURBO DNase (Fisher) and was purified with RNA Clean &
185 Concentrator-5 kit (ZYMO) following Qubit RNA High Sensitivity Kit (Invitrogen)
186 quantification. The purified RNA was used to generate the standard curve and quantify Zika
187 RNA loads as we previously described [27,29]. Zika virus RNA copies were expressed per 100
188 ng of total RNA. Strict precautions were taken to prevent PCR contamination. All master mix
189 preparations were done in the dedicated PCR cabinet. Aerosol-resistant filter pipette tips and
190 disposable gloves were used. Kit reagent controls were included in every RNA extraction and
191 PCR run.
192

193 **Cytopathic effect kinetics in wild-type and ZAP knockout cells**

194 VERO-ZAP-WT and VERO-ZAP-KO cells were seeded in 6-well plates in DMEM
195 supplemented with 10% FBS. After 24 h, the cell culture medium was removed, and monolayers
196 were gently washed twice with 1× PBS. Cell monolayers were then mock-infected or infected (3
197 replicates) with wild-type Zika virus H/2013/PF at an MOI of 1 in 1 mL of DMEM and plates
198 were incubated at 37 °C for 2 h in a CO_2 incubator. Following the incubation period, the
199 inoculum was removed, and monolayers were washed twice with 1× PBS. Subsequently, 3 mL
200 of DMEM supplemented with 2% FBS was added to each well, and plates were further incubated
201 at 37°C in a CO_2 incubator. Cells were observed under a light microscope for any visible
202 cytopathic effect.
203

204 **Statistics**

205 Zika RNA loads in VERO-ZAP-WT and VERO-ZAP-KO cells were compared using an
206 unpaired t-test. A P-value < 0.05 was considered statistically significant.

207

208 **RESULTS**

209 **ZAP affects intracellular loads of Zika virus RNA**

210 We infected VERO-ZAP-WT and VERO-ZAP-KO (**Fig 1A**) with an MOI 1 of Zika virus, and
211 sampled control (4-6 well replicates) and infected (6 well replicates) cells at 24 h and 72 h. We
212 compared viral RNA loads between WT and ZAP-KO cells with the Zika-specific RT-qPCR. At
213 24 h post-inoculation, there was no significant difference in Zika virus intracellular RNA loads;
214 however, VERO-ZAP-KO cells showed a trend towards higher RNA loads (**Fig 1B**). At 72 h
215 post-inoculation, Zika virus intracellular RNA loads were significantly higher in VERO-ZAP-
216 KO cells (**Fig 1B**).

217

218 **ZAP affects global cellular gene expression during Zika virus infection**

219 How ZAP affects global gene expression in response to virus infection was unknown. Initially,
220 we conducted simple pairwise comparisons of differentially expressed genes (DEGs). First, we
221 compared global gene expression between mock-infected VERO-ZAP-WT and VERO-ZAP-KO
222 cells: 758 and 992 genes were differently expressed between two cell lines at 24 and 72 h (**Fig**
223 **2A**; **Tables S2A, B**). Among the top ten affected genes at 24 h and 72 h (**Table S2A, B**) was
224 only one upregulated gene with known innate immunity or apoptosis function—CXCL12 (**Fig**
225 **2A**). This contrasts with affected top genes in infected cells described below.

226 Second, we compared global gene expression between mock-infected and Zika-infected VERO-
227 ZAP-WT cells: 40 and 117 genes were affected by infection at 24 h and 72 h (**Fig 2B**; **Tables**
228 **S2E, F**). Among the top ten affected genes (**Tables S2E, F**) were four genes with known innate
229 immunity or apoptosis functions—CXCL10, EGR1, G0S2, and CCL2 at 24 h, and seven
230 genes—CCL2, G0S2, CXCL10, IFNL1, OASL, CXCL8, and IL1A at 72 h. All these genes were
231 upregulated in Zika virus-infected ZAP-WT cells (**Fig 2B**).
232 Third, we compared global gene expression between mock-infected and Zika-infected VERO-
233 ZAP-KO cells: 14 and 342 genes were affected by infection at 24 h and 72 h (**Fig 2C**; **Tables**
234 **S2I, J**). Among the top ten affected genes (**Table S2I, J**) were four genes with known innate
235 immunity or apoptosis functions— EGR1, IL1A, FOS, and EGR2 at 24 h, and five genes—
236 G0S2, CCL2, CXCL10, IFNL1, and OASL at 72 h. All these genes were upregulated in Zika
237 virus-infected ZAP-KO cells (**Fig 2C**).
238
239 To further extend analysis beyond pairwise comparisons of DEGs, we conducted GO analysis.
240 This method offers high sensitivity due to its robust annotation framework, standardized
241 terminology, hierarchical structure, integration with biological knowledge, continuous updates,
242 and statistical rigor where each gene in the entire input set (**Table S1**) is statistically processed
243 and used for annotation [44,45].
244 Along with profound gene expression changes, mock-infected VERO-ZAP-WT and VERO-
245 ZAP-KO cells had 92 (24 h) and 178 (72 h) significantly affected GO biological processes
246 (**Tables S2C, D**). However, when we searched among affected GO biological processes
247 keywords—"viral/virus", "apoptotic/apoptosis", "immun*", and "interferon," we did not find
248 affected processes containing these keywords. This sharply contrasts with affected GO biological

249 processes in infected cells described below. Zika-infected VERO-ZAP-WT cells had 303 (24 h)
250 and 864 (72 h) affected GO biological processes (**Tables S2G, H**). Zika-infected VERO-ZAP-
251 KO cells had 287 (24 h) and 384 (72 h) affected GO biological processes (**Tables S2K, L**).
252 We narrowed down analysis and compared GO biological processes related to virus infection in
253 VERO-ZAP-WT and VERO-ZAP-KO cells at 24 and 72 h. As expected, no affected "viral" GO
254 processes were detected in mock-infected control cells (**Fig 3A**). Infected VERO-ZAP-WT cells
255 showed 5 affected processes at 24 h, and the number increased at 72 h reaching 16 affected
256 processes (**Fig 3B**). In contrast, infected VERO-ZAP-KO cells showed no affected processes at
257 24 h, and the number increased at 72 h reaching only 5 affected processes (**Fig 3C**).
258 We also compared GO biological processes related to immune responses in VERO-ZAP-WT and
259 VERO-ZAP-KO cells at 24 and 72 h. As expected, no affected "immune*" GO processes were
260 detected in mock-infected control cells (**Fig 4A**). Infected VERO-ZAP-WT cells showed one
261 affected process at 24 h, and the number increased at 72 h reaching 16 affected processes (**Fig**
262 **4B**). Infected VERO-ZAP-KO cells showed one affected process at 24 h, and the number
263 increased at 72 h reaching only 4 affected processes (**Fig 4C**).
264 Affected GO biological processes related to apoptosis in VERO-ZAP-WT and VERO-ZAP-KO
265 cells (**Fig S1**) had the same patterns as "viral" and "immune" processes (**Figs 3, 4**). No affected
266 "apoptosis" GO processes were detected in mock-infected control cells (**Fig S1A**). Infected
267 VERO-ZAP-WT cells showed 5 affected processes at 24 h, and the number increased at 72 h
268 reaching 24 affected processes (**Fig S1B**). In contrast, infected VERO-ZAP-KO cells showed
269 only 2 affected processes at 24 h, and the number increased at 72 h reaching only 9 affected
270 processes (**Fig S1C**).
271

272 More aggressive "viral" responses to infection in VERO-ZAP-WT cells than in VERO-ZAP-KO
273 cells at 24 h identified by GO analysis (**Fig 3B**, **C**) may determine the higher number of affected
274 "apoptosis" GO processes in VERO-ZAP-WT cells (**Fig S1B**, **C**) because antiviral
275 transcriptional responses and cell death are interconnected and are critical components of the
276 host response to virus infection [46,47]. Many innate immune signaling pathways can promote
277 cell death [46,47]. In contrast to the signaling pathways that promote antiviral transcription,
278 those that initiate cell death following virus infection remain less understood [46]. To probe
279 whether ZAP affects cell death during Zika infection in VERO cells, we compared cytopathic
280 effects (CPE) in VERO-ZAP-WT and VERO-ZAP-KO cells. We infected VERO-ZAP-WT and
281 VERO-ZAP-KO in the same way as in the RNA-seq experiment with an MOI 1 of Zika virus. At
282 24 h, VERO-ZAP-KO cells did not show visible CPE (**Fig S2**). In contrast, VERO-ZAP-WT
283 cells showed prominent CPE at 24 h—diffuse focies of detached cells (**Fig S2**). At 30 h, the
284 difference was prominent, CPE in VERO-ZAP-WT aggravated to diffuse cell detachment, but
285 VERO-ZAP-KO cells did not display visible CPE until 48 h post-infection (**Fig S2**). At 48 h and
286 72 h, both cell lines had similar diffused cell detachment; however, continuous cell monolayers
287 were mostly preserved. This CPE pattern aggravated at 96 h, where VERO-ZAP-WT had a lot of
288 dead cells but still maintained preserved monolayer, and VERO-ZAP-KO had many dead cells
289 with many spots of disrupted monolayer. At 120 h, the monolayers were mostly disrupted in both
290 cell lines. This difference in CPE progression in wild-type and ZAP-KO cells suggests a role for
291 ZAP in modulating cell death during Zika virus infection.
292
293 Taken together, the viral RNA loads, RNA-seq data, and cell death patterns support our
294 hypothesis that a more robust, potentially ZAP-mediated, antiviral response in VERO-ZAP-WT

295 cells compared to VERO-ZAP-KO cells (**Figs 3, 4; Fig S1**) more effectively controls Zika virus
296 infection (**Fig 1B**) but leads to heightened cell death during early infection (24-48 hours; **Fig S2**).
297 As infection progresses (**72-96 hours**), immune responses in ZAP-WT cells continue controlling
298 Zika virus infection (**Fig 1B**), while the less controlled infection in ZAP-KO cells (**Fig 1B**)
299 contributes to more extensive cell lysis (**Fig S2**). Further studies are needed to validate this
300 hypothesis and gain a better understanding of the molecular interplay between ZAP-mediated
301 antiviral responses and cell death.
302

303 **DISCUSSION**

304 The zinc finger CCCH-type antiviral protein 1 is an interferon (IFN)-stimulated gene (ISG) [1-
305 5]. Also, there are conflicting studies regarding the capacity of ZAP to enhance the type I IFN
306 antiviral response [5,48-50]. Here, we found that during Zika infection, endogenous ZAP was
307 associated with amplification of global transcriptional antiviral and immune responses in VERO
308 cells which are deficient in IFN-α/β [4,51]. We do not know yet how these type I IFN-
309 independent antiviral cellular responses associated with endogenous ZAP work. ZAP knockout
310 also considerably impacted global gene expression in uninfected cells; however, GO processes
311 related to antiviral, immune, and apoptosis events were not identified suggesting the specificity
312 of findings in Zika-infected cells.
313

314 Our study is confined to a single VERO-ZAP-KO clone, and conducting additional tests using
315 multiple clones could yield further insights. Such an endeavor falls beyond the scope of this
316 study; however, our RNA-seq results find indirect support from previous research conducted on
317 different uninfected wild-type and ZAP-KO cell lines. Specifically, global gene expression

318 analysis with Agilent microarrays revealed 1,065 upregulated and 776 downregulated transcripts
319 in uninfected wild-type and ZAP-KO HeLa cells [43]. Another study using RNA-seq identified a
320 number of DEGs between uninfected ZAP-WT and ZAP-KO A549 cells [52]. In the most recent
321 study, the authors demonstrated that ZAP influences hundreds of transcripts in ZAP-WT and
322 ZAP-KO HEK cells [53]. Directly comparing the DEGs between our study and the above studies
323 poses challenges due to variations in cell types, origins, and the employed comparative
324 bioinformatics strategies. Nonetheless, the overarching trend in all previous studies strongly
325 corroborates significant transcriptional differences between non-infected ZAP-WT and ZAP-KO
326 VERO cells (**Fig 2A; Tables S2A-D**).
327
328 The above studies did not use virus infection for RNA-seq comparison between ZAP-WT and
329 ZAP-KO cells. Thus, our study provides the first high-throughput dataset highlighting the impact
330 of ZAP on global gene expression during virus infection. During submission of this manuscript,
331 a study indirectly supporting our findings was published [53]. The authors used RNA-seq in
332 ZAP-WT and ZAP-KO HEK cells transfected with viral mimetic RNA oligos and mock
333 transfection to normalize DEGs. From this study, we used the top 16 innate immune response
334 genes (**Table S2M**) overexpressed in ZAP-WT HEK cells as compared to ZAP-KO for
335 comparative purposes. At 24 h, two genes in this HEK list (**Table S2M**)—IFIT1 and ISG15—
336 were upregulated in Zika virus-infected VERO-ZAP-WT cells as compared to mock control
337 VRO-ZAP-WT cells (**Table S2E;** highlighted). In contrast, no genes from the HEK list were
338 affected in Zika virus-infected VERO-ZAP-KO cells (**Table S2I**). At 72 h, eight-nine innate
339 immune response genes in the list (**Table S2M**) were upregulated in both Zika virus-infected
340 VEO-ZAP-WT and VERO-ZAP-KO cells (**Table S2F, J**); but comparison at 72 h is not

341 sufficiently informative because previous HEK study was only conducted at 24 h after
342 transfection. Nonetheless, this pattern of ZAP-dependent affected genes, where ZAP-WT cells
343 show innate immune responses earlier than ZAP-KO cells, is in accordance with our GO analysis
344 (**Figs 3, 4**).
345 We do not see a complete match between the previous HEK (**Table S2M**) and our VERO
346 dataset; not all genes identified as upregulated in transfected ZAP-WT HEK cells were
347 significantly upregulated in infected VERO-ZAP-WT cells (**Table S2E, I, F, J**). This
348 discrepancy may be explained by the type I IFN competency of HEK cells and the deficiency of
349 VERO cells. Nonetheless, two important innate immune genes—IFIT1 and ISG15—were
350 upregulated in transfected or infected ZAP-WT cells in both studies, suggesting their ZAP-
351 mediated augmentation in the absence of the type I IFN system. Potential type I IFN-independent
352 and -dependent interactions between ZAP and IFIT1 are of particular interest because ZAP and
353 IFIT1 together have recently been identified to constitute the majority of IFN-mediated
354 restriction of alphavirus, specifically Venezuelan equine encephalitis virus [26].
355
356 The previous ZAP study showed JEV sensitivity to ectopic ZAP, and insensitivity of Zika virus
357 [7]. The discrepancy between previous and present studies may be explained by different
358 experimental approaches. The previous study involved the overexpression of ectopic ZAP in
359 ZAP-positive cells [7], whereas our study compared Zika RNA loads between ZAP-WT and
360 ZAP-KO cells. Additionally, different cell lines were used: A549 cells from human cancer lung
361 tissue in the previous study [7], and VERO cells from a healthy monkey in our study. Antiviral
362 signaling can vary significantly between different cell types [2,56]. Another potential factor is
363 that human cells were used previously, and here we used the cell line derived from a healthy

364 adult African green monkey—a possible natural reservoir host of Zika virus [57]. Moreover,
365 while the previous study used 10-hour and 24-hour sampling times, we conducted RT-qPCR and
366 RNA-seq at 24 h and 72 h after Zika infection, revealing delayed effects, indicative of indirect
367 ZAP-mediated antiviral activity.
368

369 **CONCLUSIONS**

370 Altogether, our preliminary study underscores the importance of ZAP in augmenting cellular
371 responses against Zika virus even in the absence of the robust type I IFN system. Further
372 investigations are warranted to elucidate the mechanisms underlying these type I IFN-
373 independent antiviral cellular responses mediated by ZAP. The considerable augmentation of
374 antiviral responses by endogenous ZAP against Zika virus highlights its potential as a therapeutic
375 target. However, comprehensive studies are required to fully understand the intricacies of ZAP-
376 mediated antiviral activity and its implications for combating Zika virus infection.
377
378

379 **DISCLOSURE STATEMENT**

380 The authors declare that the research was conducted in the absence of any commercial or
381 financial relationships that could be construed as a potential conflict of interest.
382
383

384 **DATA AVAILABILITY**

385 Raw RNA-seq files are deposited to NCBI BioProject (PRJNA1101086).
386
387

FUNDING

PPS received a Scholarship from the School of Public Health, University of Saskatchewan**.** This work was partially supported by a grant to UK from the Canadian Institutes of Health Research (CIHR; Project Grant #424307). The funders had no role in study design, data collection and analysis, decision to publish, or manuscript preparation.

411 **REFERENCES**

412 1. Nguyen LP, Aldana KS, Yang E, et al. Alphavirus Evasion of Zinc Finger Antiviral Protein (ZAP)
413 Correlates with CpG Suppression in a Specific Viral nsP2 Gene Sequence. Viruses. 2023 Mar
414 24;15(4).
415 2. MacDonald MR, Machlin ES, Albin OR, et al. The zinc finger antiviral protein acts synergistically
416 with an interferon-induced factor for maximal activity against alphaviruses. J Virol. 2007
417 Dec;81(24):13509-18.
418 3. Li MMH, Aguilar EG, Michailidis E, et al. Characterization of Novel Splice Variants of Zinc Finger
419 Antiviral Protein (ZAP). J Virol. 2019 Sep 15;93(18).
420 4. Crosse KM, Monson EA, Beard MR, et al. Interferon-Stimulated Genes as Enhancers of Antiviral
421 Innate Immune Signaling. J Innate Immun. 2018;10(2):85-93.
422 5. Hayakawa S, Shiratori S, Yamato H, et al. ZAPS is a potent stimulator of signaling mediated by
423 the RNA helicase RIG-I during antiviral responses. Nat Immunol. 2011 Jan;12(1):37-44.
424 6. Zhu Y, Gao G. ZAP-mediated mRNA degradation. RNA Biol. 2008 Apr-Jun;5(2):65-7.
425 7. Chiu HP, Chiu H, Yang CF, et al. Inhibition of Japanese encephalitis virus infection by the host
426 zinc-finger antiviral protein. PLoS Pathogens: Public Library of Science; 2018.
427 8. Ye P, Liu S, Zhu Y, et al. DEXH-Box protein DHX30 is required for optimal function of the zinc-
428 finger antiviral protein. Protein Cell. 2010 Oct;1(10):956-64.
429 9. Chen G, Guo X, Lv F, et al. p72 DEAD box RNA helicase is required for optimal function of the
430 zinc-finger antiviral protein. Proc Natl Acad Sci U S A. 2008 Mar 18;105(11):4352-7.
431 10. Li MM, Lau Z, Cheung P, et al. TRIM25 Enhances the Antiviral Action of Zinc-Finger Antiviral
432 Protein (ZAP). PLoS Pathog. 2017 Jan;13(1):e1006145.
433 11. Zheng X, Wang X, Tu F, et al. TRIM25 Is Required for the Antiviral Activity of Zinc Finger Antiviral
434 Protein. Journal of virology: J Virol; 2017.
435 12. Ficarelli M, Wilson H, Pedro Galão R, et al. KHNYN is essential for the zinc finger antiviral protein
436 (ZAP) to restrict HIV-1 containing clustered CpG dinucleotides. eLife2019.
437 13. Buckmaster MV, Goff SP. Riplet Binds the Zinc Finger Antiviral Protein (ZAP) and Augments ZAP-
438 Mediated Restriction of HIV-1. Journal of Virology: American Society for Microbiology; 2022.
439 14. Gao G, Guo X, Goff SP. Inhibition of retroviral RNA production by ZAP, a CCCH-type zinc finger
440 protein. Science (New York, N.Y.): American Association for the Advancement of Science; 2002.
441 p. 1703-6.
442 15. Bick MJ, Carroll JW, Gao G, et al. Expression of the zinc-finger antiviral protein inhibits alphavirus
443 replication. J Virol. 2003 Nov;77(21):11555-62.
444 16. Liu CH, Zhou L, Chen G, et al. Battle between influenza A virus and a newly identified antiviral
445 activity of the PARP-containing ZAPL protein. Proc Natl Acad Sci U S A. 2015 Nov
446 10;112(45):14048-53.
447 17. Mao R, Nie H, Cai D, et al. Inhibition of hepatitis B virus replication by the host zinc finger
448 antiviral protein. PLoS Pathog. 2013;9(7):e1003494.
449 18. Muller S, Moller P, Bick MJ, et al. Inhibition of filovirus replication by the zinc finger antiviral
450 protein. J Virol. 2007 Mar;81(5):2391-400.
451 19. Tang Q, Wang X, Gao G. The Short Form of the Zinc Finger Antiviral Protein Inhibits Influenza A
452 Virus Protein Expression and Is Antagonized by the Virus-Encoded NS1. J Virol. 2017 Jan
453 15;91(2).
454 20. Zhu Y, Chen G, Lv F, et al. Zinc-finger antiviral protein inhibits HIV-1 infection by selectively
455 targeting multiply spliced viral mRNAs for degradation. Proc Natl Acad Sci U S A. 2011 Sep
456 20;108(38):15834-9.

457 21. Takata MA, Goncalves-Carneiro D, Zang TM, et al. CG dinucleotide suppression enables antiviral
458 defence targeting non-self RNA. Nature. 2017 Oct 5;550(7674):124-127.
459 22. Miyazato P, Matsuo M, Tan BJY, et al. HTLV-1 contains a high CG dinucleotide content and is
460 susceptible to the host antiviral protein ZAP. Retrovirology. 2019 Dec 16;16(1):38.
461 23. Gonzalez-Perez AC, Stempel M, Wyler E, et al. The Zinc Finger Antiviral Protein ZAP Restricts
462 Human Cytomegalovirus and Selectively Binds and Destabilizes Viral UL4/UL5 Transcripts. mBio.
463 2021 May 4;12(3).
464 24. Zhao Y, Song Z, Bai J, et al. ZAP, a CCCH-Type Zinc Finger Protein, Inhibits Porcine Reproductive
465 and Respiratory Syndrome Virus Replication and Interacts with Viral Nsp9. J Virol. 2019 May
466 15;93(10).
467 25. Xie L, Lu B, Zheng Z, et al. The 3C protease of enterovirus A71 counteracts the activity of host
468 zinc-finger antiviral protein (ZAP). J Gen Virol. 2018 Jan;99(1):73-85.
469 26. McDougal MB, De Maria AM, Ohlson MB, et al. Interferon inhibits a model RNA virus via a
470 limited set of inducible effector genes. EMBO Rep. 2023 Sep 6;24(9):e56901.
471 27. Trus I, Udenze D, Berube N, et al. CpG-Recoding in Zika Virus Genome Causes Host-Age-
472 Dependent Attenuation of Infection With Protection Against Lethal Heterologous Challenge in
473 Mice. Front Immunol. 2019;10:3077.
474 28. Trus I, Berube N, Jiang P, et al. Zika Virus with Increased CpG Dinucleotide Frequencies Shows
475 Oncolytic Activity in Glioblastoma Stem Cells. Viruses: Multidisciplinary Digital Publishing
476 Institute; 2020. p. 579.
477 29. Udenze D, Trus I, Berube N, et al. The African strain of Zika virus causes more severe in utero
478 infection than Asian strain in a porcine fetal transmission model. Emerging Microbes &
479 Infections. 2019; 8:1098-1107.2019.
480 30. Darbellay J, Cox B, Lai K, et al. Zika Virus Causes Persistent Infection in Porcine Conceptuses and
481 may Impair Health in Offspring. EBioMedicine. 25:73-86.2017.
482 31. Trus I, Udenze D, Cox B, et al. Subclinical in utero Zika virus infection is associated with
483 interferon alpha sequelae and sex-specific molecular brain pathology in asymptomatic porcine
484 offspring. In: Pierson TC, editor. PLoS Pathogens2019. p. e1008038.
485 32. Udenze D, Trus I, Lipsit S, et al. Offspring affected with in utero Zika virus infection retain
486 molecular footprints in the bone marrow and blood cells. Emerging microbes & infections:
487 Emerg Microbes Infect; 2022. p. 1-43.
488 33. Chapagain S, Pal Singh P, Le K, et al. Japanese encephalitis virus persists in the human
489 reproductive epithelium and porcine reproductive tissues. PLoS Negl Trop Dis. 2022
490 Jul;16(7):e0010656.
491 34. Bray NL, Pimentel H, Melsted P, et al. Near-optimal probabilistic RNA-seq quantification. Nature
492 Biotechnology. 2016 2016/05/01;34(5):525-527.
493 35. Warren WC, Jasinska AJ, Garcia-Perez R, et al. The genome of the vervet (Chlorocebus aethiops
494 sabaeus). Genome Res. 2015 Dec;25(12):1921-33.
495 36. Law CW, Alhamdoosh M, Su S, et al. RNA-seq analysis is easy as 1-2-3 with limma, Glimma and
496 edgeR. F1000Res. 2016;5.
497 37. Raudvere U, Kolberg L, Kuzmin I, et al. g:Profiler: a web server for functional enrichment analysis
498 and conversions of gene lists (2019 update). Nucleic Acids Res. 2019 Jul 2;47(W1):W191-W198.
499 38. Li H, Durbin R. Fast and accurate short read alignment with Burrows-Wheeler transform.
500 Bioinformatics. 2009 Jul 15;25(14):1754-60.
501 39. Sabir AJ, Singh PP, Trus I, et al. Asian Zika virus can acquire generic African-lineage mutations
502 during in utero infection. Emerg Microbes Infect. 2023 Dec;12(2):2263592.
503 40. Udenze D, Trus I, Berube N, et al. CpG content in the Zika virus genome affects infection
504 phenotypes in the adult brain and fetal lymph nodes. Front Immunol. 2022;13:943481.

505 41. Udenze D, Trus I, Munyanduki H, et al. The isolated in utero environment is conducive to the
506 emergence of rna and dna virus variants. Viruses: Multidisciplinary Digital Publishing Institute;
507 2021. p. 1827.
508 42. Xu MY, Liu SQ, Deng CL, et al. Detection of Zika virus by SYBR green one-step real-time RT-PCR.
509 Journal of virological methods: J Virol Methods; 2016. p. 93-97.
510 43. Todorova T, Bock FJ, Chang P. PARP13 regulates cellular mRNA post-transcriptionally and
511 functions as a pro-apoptotic factor by destabilizing TRAILR4 transcript. Nature communications.
512 2014 Nov 10;5:5362.
513 44. The Gene Ontology C. The Gene Ontology Resource: 20 years and still GOing strong. Nucleic
514 Acids Res. 2019 Jan 8;47(D1):D330-D338.
515 45. Ashburner M, Ball CA, Blake JA, et al. Gene ontology: tool for the unification of biology. The
516 Gene Ontology Consortium. Nat Genet. 2000 May;25(1):25-9.
517 46. Orzalli MH, Kagan JC. Apoptosis and Necroptosis as Host Defense Strategies to Prevent Viral
518 Infection. Trends Cell Biol. 2017 Nov;27(11):800-809.
519 47. Upton JW, Chan FK. Staying alive: cell death in antiviral immunity. Mol Cell. 2014 Apr
520 24;54(2):273-80.
521 48. Schwerk J, Soveg FW, Ryan AP, et al. RNA-binding protein isoforms ZAP-S and ZAP-L have distinct
522 antiviral and immune resolution functions. Nat Immunol. 2019 Dec;20(12):1610-1620.
523 49. Lee H, Komano J, Saitoh Y, et al. Zinc-finger antiviral protein mediates retinoic acid inducible
524 gene I-like receptor-independent antiviral response to murine leukemia virus. Proc Natl Acad Sci
525 U S A. 2013 Jul 23;110(30):12379-84.
526 50. Kozaki T, Takahama M, Misawa T, et al. Role of zinc-finger anti-viral protein in host defense
527 against Sindbis virus. Int Immunol. 2015 Jul;27(7):357-64.
528 51. Emeny JM, Morgan MJ. Regulation of the interferon system: evidence that Vero cells have a
529 genetic defect in interferon production. J Gen Virol. 1979 Apr;43(1):247-52.
530 52. Shaw AE, Rihn SJ, Mollentze N, et al. The antiviral state has shaped the CpG composition of the
531 vertebrate interferome to avoid self-targeting. PLoS Biol. 2021 Sep;19(9):e3001352.
532 53. Busa VF, Ando Y, Aigner S, et al. Transcriptome regulation by PARP13 in basal and antiviral states
533 in human cells. iScience. 2024 Apr 19;27(4):109251.
534 54. Caine EA, Scheaffer SM, Arora N, et al. Interferon lambda protects the female reproductive tract
535 against Zika virus infection. Nature Communications 2019 10:1: Nature Publishing Group; 2019.
536 p. 1-12.
537 55. Karki S, Li MM, Schoggins JW, et al. Multiple interferon stimulated genes synergize with the zinc
538 finger antiviral protein to mediate anti-alphavirus activity. PLoS One. 2012;7(5):e37398.
539 56. Pallett MA, Lu Y, Smith GL. DDX50 Is a Viral Restriction Factor That Enhances IRF3 Activation.
540 Viruses. 2022 Feb 3;14(2).
541 57. Buechler CR, Bailey AL, Weiler AM, et al. Seroprevalence of Zika Virus in Wild African Green
542 Monkeys and Baboons. mSphere. 2017 Mar-Apr;2(2).

543

544

545

546

547 **FIGURE LEGENDS**

548

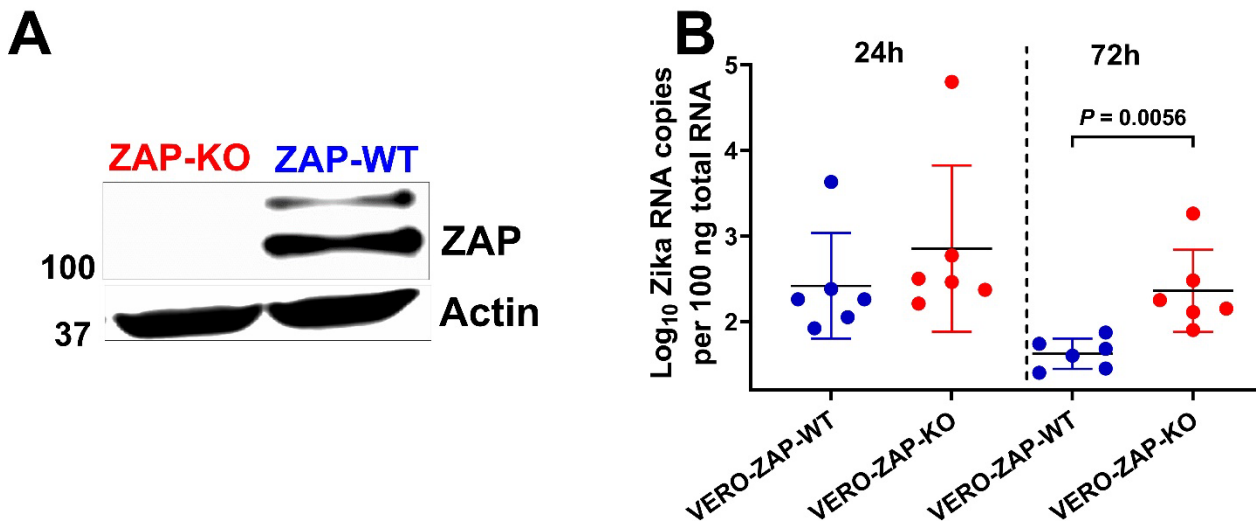

549

550 **Fig 1. Infection phenotypes of Zika virus in wild-type (VERO-ZAP-WT) and ZAP knockout**
551 **(VERO-ZAP-KO) cells.** (**A**) ZAP western blot. KO status was also confirmed by Sanger
552 sequencing. (**B**) Reduced intracellular Zika virus RNA in VERO-ZAP-WT cells at 24 h and 72 h,
553 MOI 1. Determined by the Zika-specific RT-qPCR assay. All mock-infected samples were
554 negative in Zika-specific RT-qPCR. Statistics—an unpaired t-test.

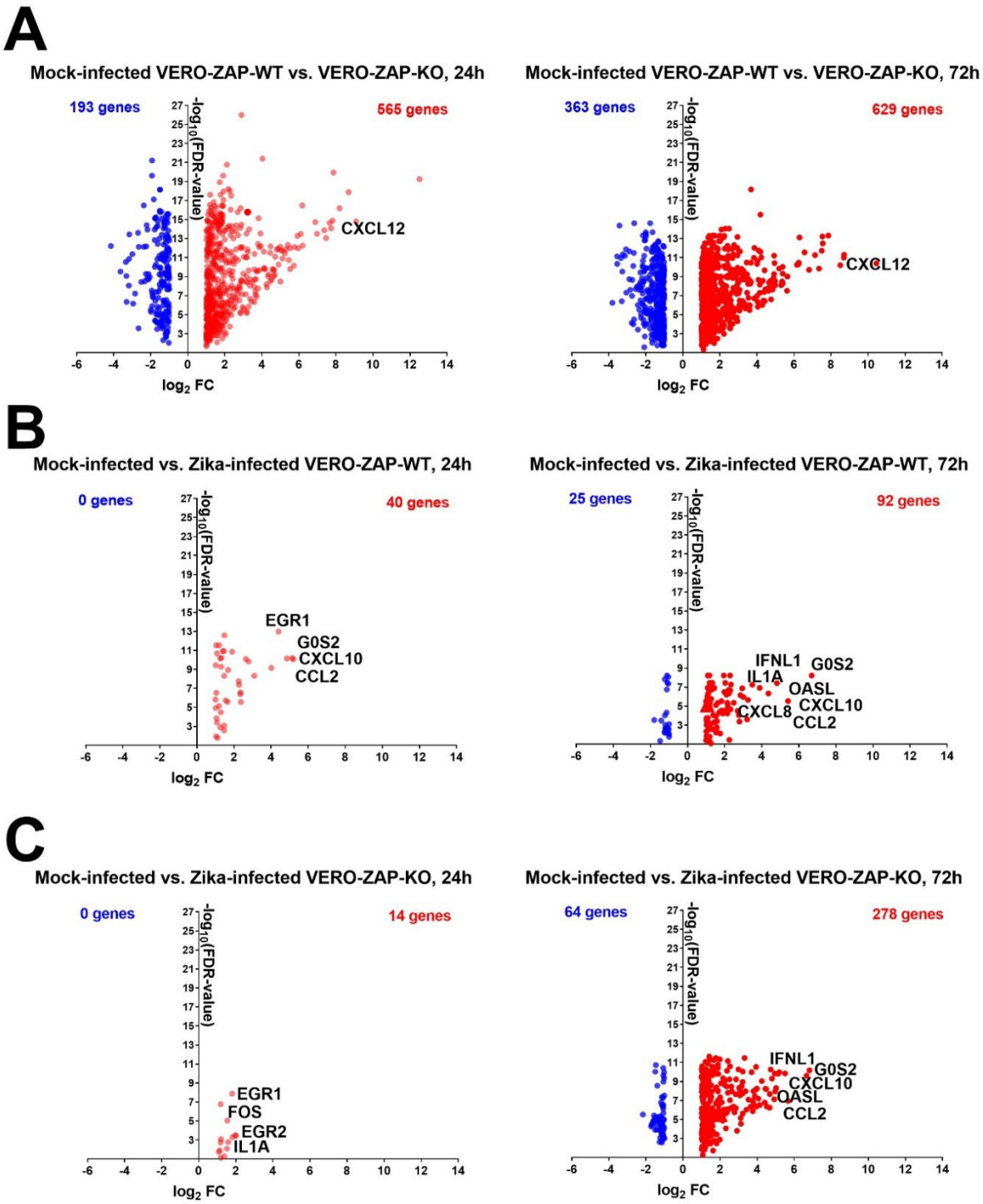

Fig 2. Cellular transcriptional gene responses during Zika virus infection. (**A**) Mock-infected ZAP-WT versus VERO-ZAP-KO cells. Direction of analysis: WT/KO. (**B**) Mock-infected versus Zika-infected VERO-ZAP-WT cells. Direction of analysis: Zika-infected/Mock-infected. (**C**) Mock-infected versus Zika-infected VERO-ZAP-KO cells. Direction of analysis: Zika-infected/Mock-infected. Plots of the upregulated (red) and downregulated (blue) genes. **FDR**: The false discovery rate. Genes with FDR < 0.05 and log2 fold change (FC) > 1 were significantly affected. The top 10 affected genes associated with innate immune response or apoptosis are shown. Raw data are in **Tables S2A, B, E, F, I, J**.

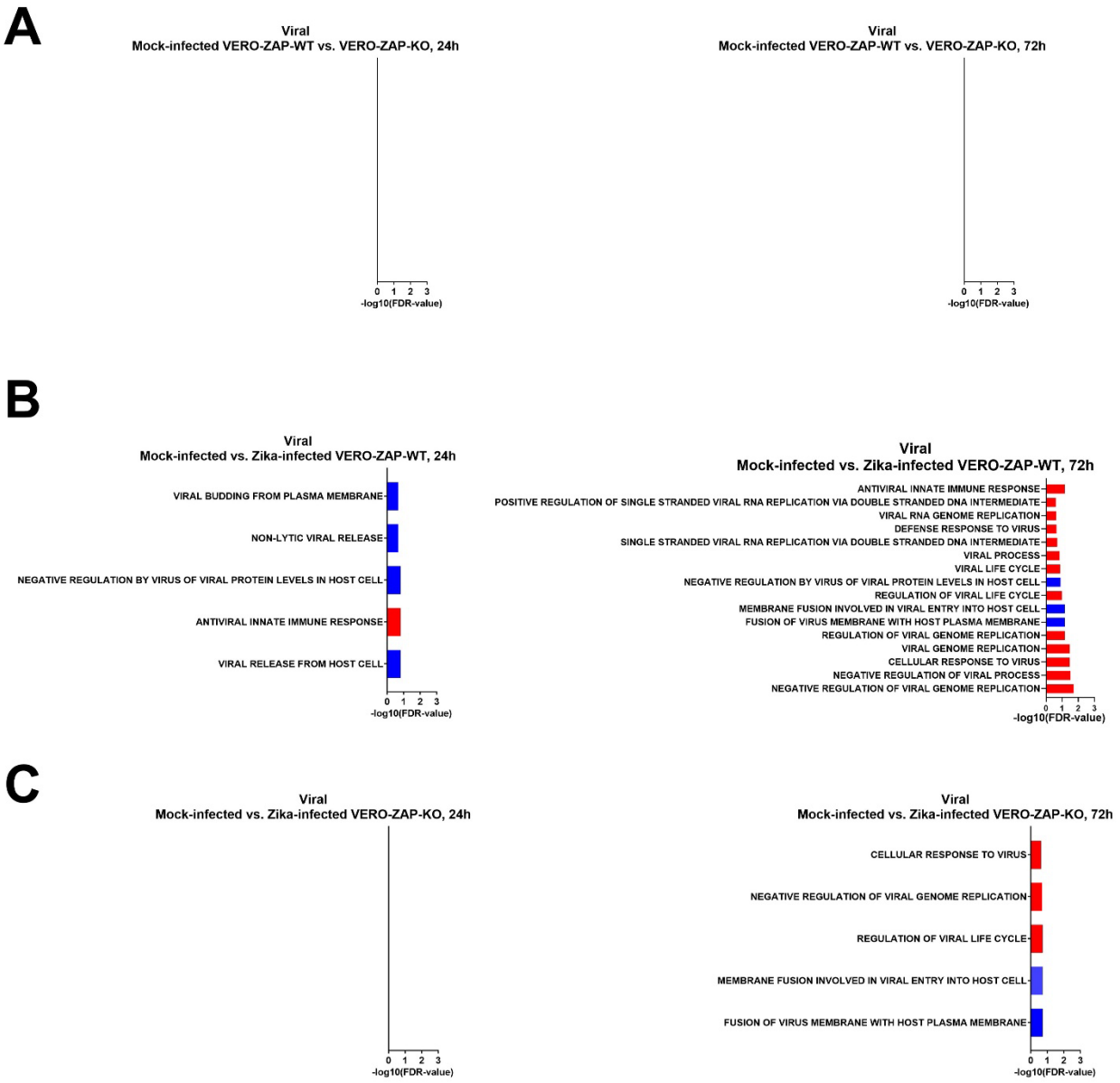

Fig 3. Biological "viral" processes affected in VERO-ZAP-WT and VERO-ZAP-KO cells at 24 h and 72 h after Zika virus infection. (**A**) Mock-infected ZAP-WT versus VERO-ZAP-KO cells. Direction of analysis: WT/KO. (**B**) Mock-infected versus Zika-infected VERO-ZAP-WT cells. Direction of analysis: Zika-infected/Mock-infected. (**C**) Mock-infected versus Zika-infected VERO-ZAP-KO cells. Direction of analysis: Zika-infected/Mock-infected. Red bars–upregulated processes. Blue bars–downregulated processes. **FDR**: The false discovery rate. Raw data are in **Tables S2C, D, G, H, K, L**.

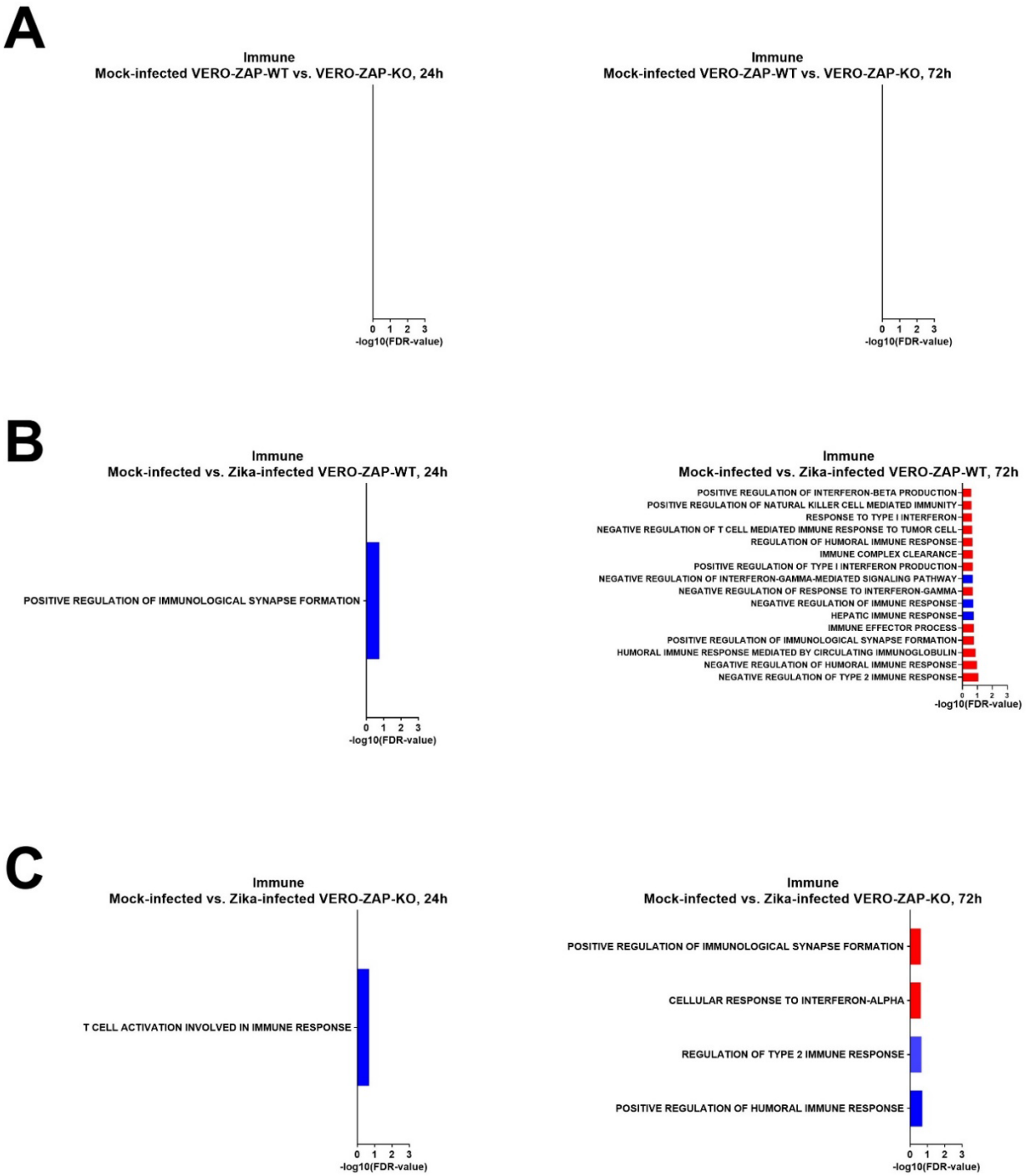

Fig 4. Biological "immune*" processes affected in VERO-ZAP-WT and VERO-ZAP-KO cells at 24 h and 72 h after Zika virus infection. (**A**) Mock-infected ZAP-WT versus VERO-ZAP-KO cells. Direction of analysis: WT/KO. (**B**) Mock-infected versus Zika-infected VERO-ZAP-WT cells. Direction of analysis: Zika-infected/Mock-infected. (**C**) Mock-infected versus Zika-infected VERO-ZAP-KO cells. Direction of analysis: Zika-infected/Mock-infected. Red bars–upregulated processes. Blue bars– downregulated processes. **FDR**: The false discovery rate. Raw data are in **Tables S2C, D, G, H, K, L**.

587 **SUPPLEMENTARY FIGURES**
588

589

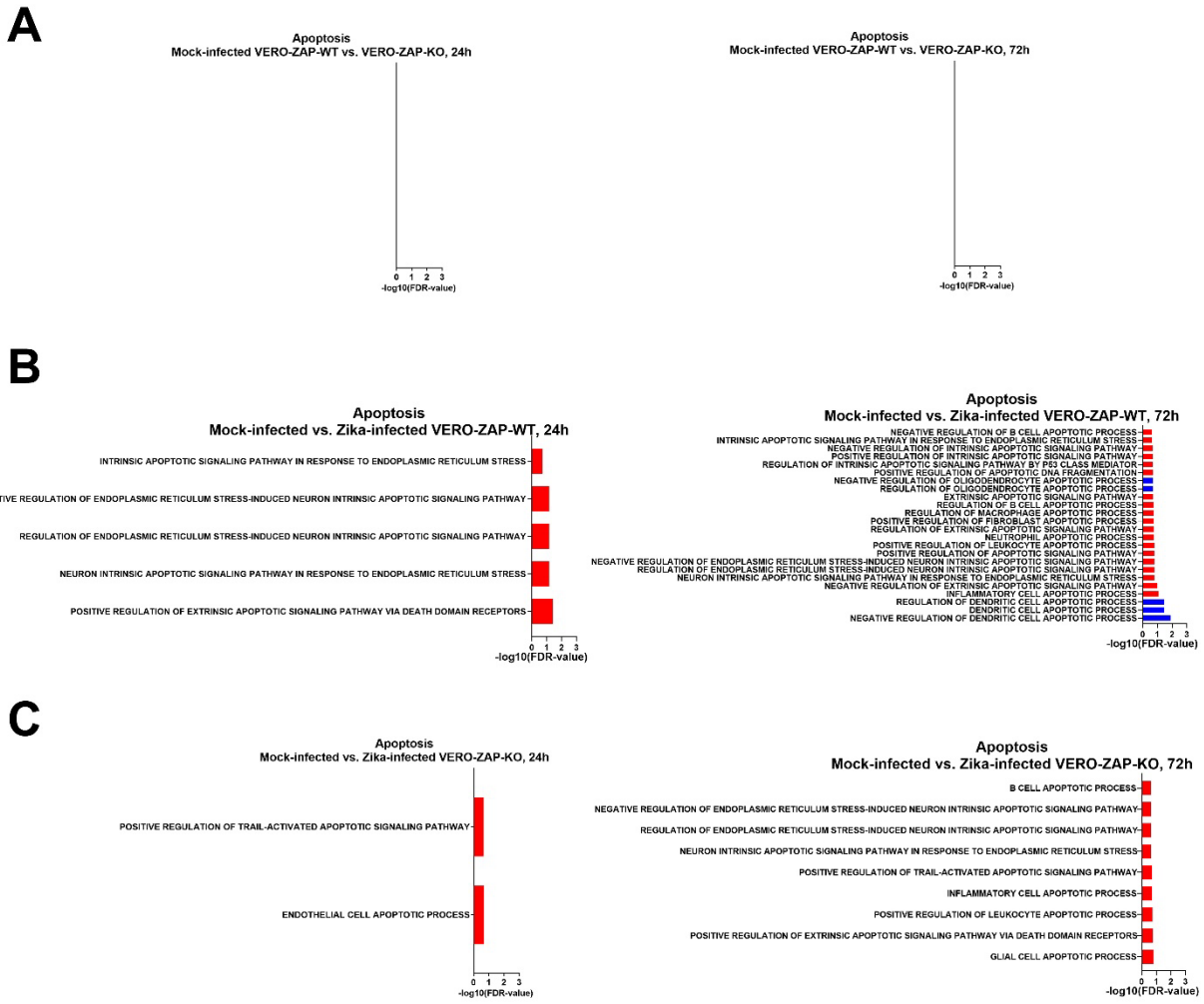

590

591 **Fig S1. Biological "apoptosis" processes affected in VERO-ZAP-WT and VERO-ZAP-KO**
592 **cells at 24 h and 72 h after Zika virus infection.** (**A**) Mock-infected ZAP-WT versus VERO-
593 ZAP-KO cells. Direction of analysis: WT/KO. (**B**) Mock-infected versus Zika-infected VERO-
594 ZAP-WT cells. Direction of analysis: Zika-infected/Mock-infected. (**C**) Mock-infected versus
595 Zika-infected VERO-ZAP-KO cells. Direction of analysis: Zika-infected/Mock-infected. Red
596 bars–upregulated processes. Blue bars- downregulated processes. **FDR**: The false discovery rate.
597 Raw data are in **Tables S2C, D, G, H, K, L**.
598
599
600
601
602
603
604
605

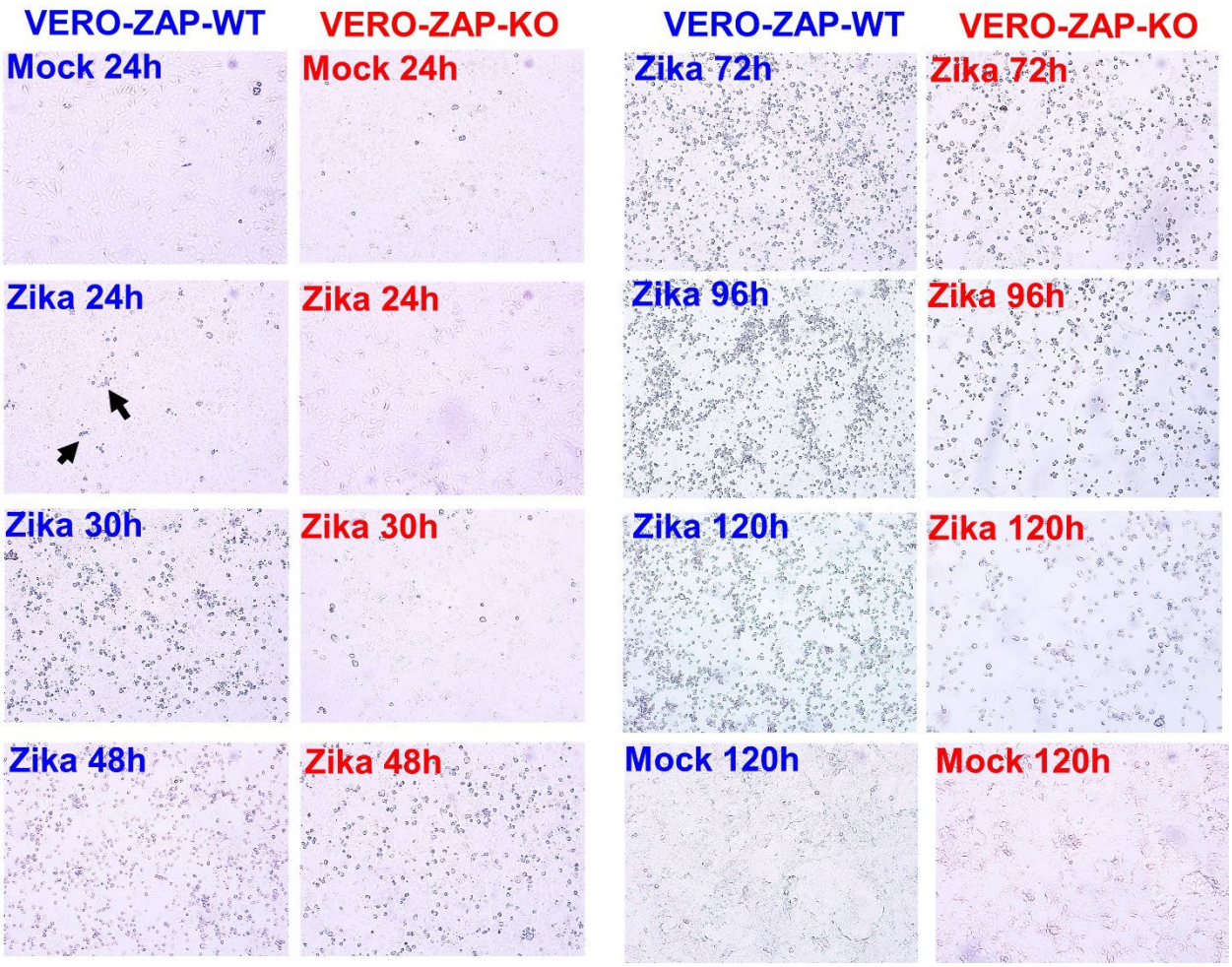

Fig S2. Cytopathic effect patterns during Zika virus infection in VERO-ZAP-WT and VERO-ZAP-KO cells, MOI 1. Arrows show diffuse small focies of detached cells. The experiment was done in three replicates for each cell line. Images represent the typical pattern in all replicates.

Table S1 Raw RNAseq data (DEGs).

Table S2 Significantly affected DEGs and GO processes.

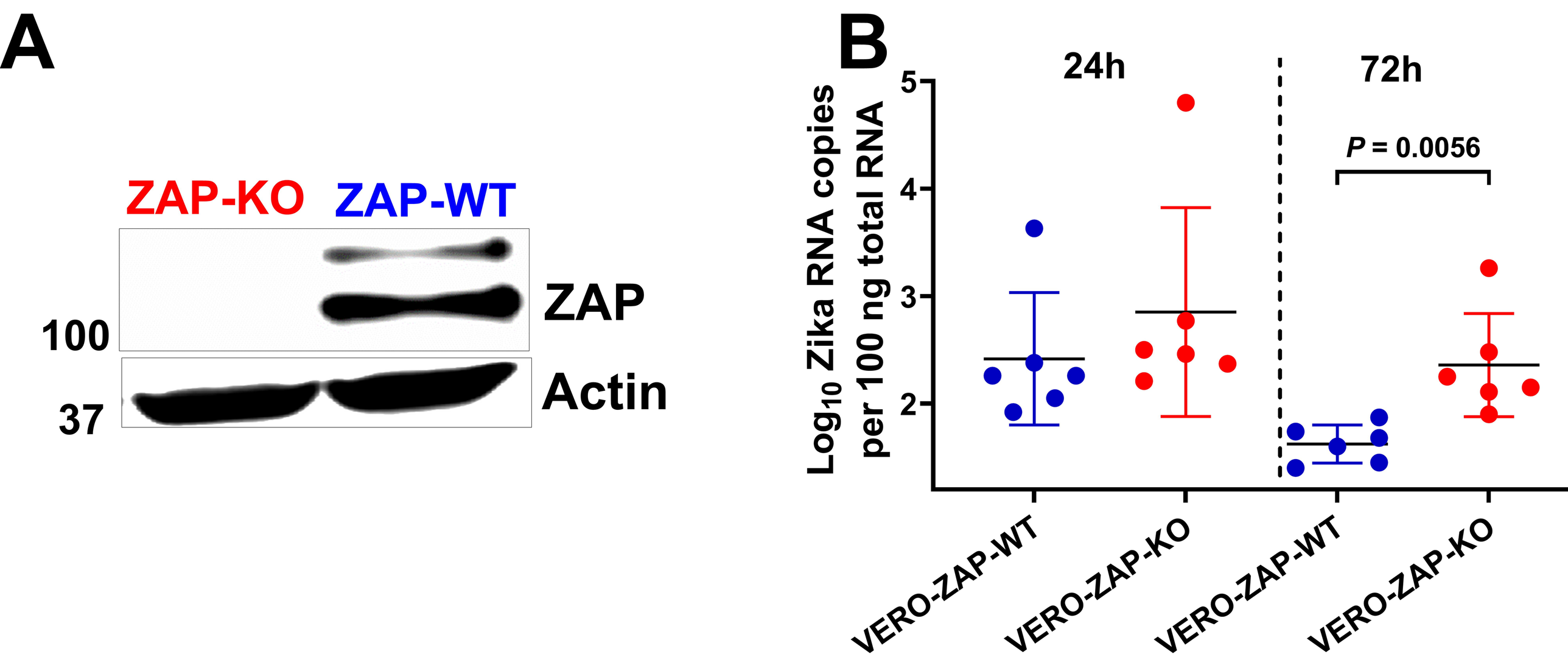
A
ZAP-KO
ZAP-WT
100
37
ZAP
Actin
B
24h
72h
P = 0.0056
Log10 Zika RNA copies per 100 ng total RNA
5
4
3
2
VERO-ZAP-WT
VERO-ZAP-KO
VERO-ZAP-WT
VERO-ZAP-KO

A

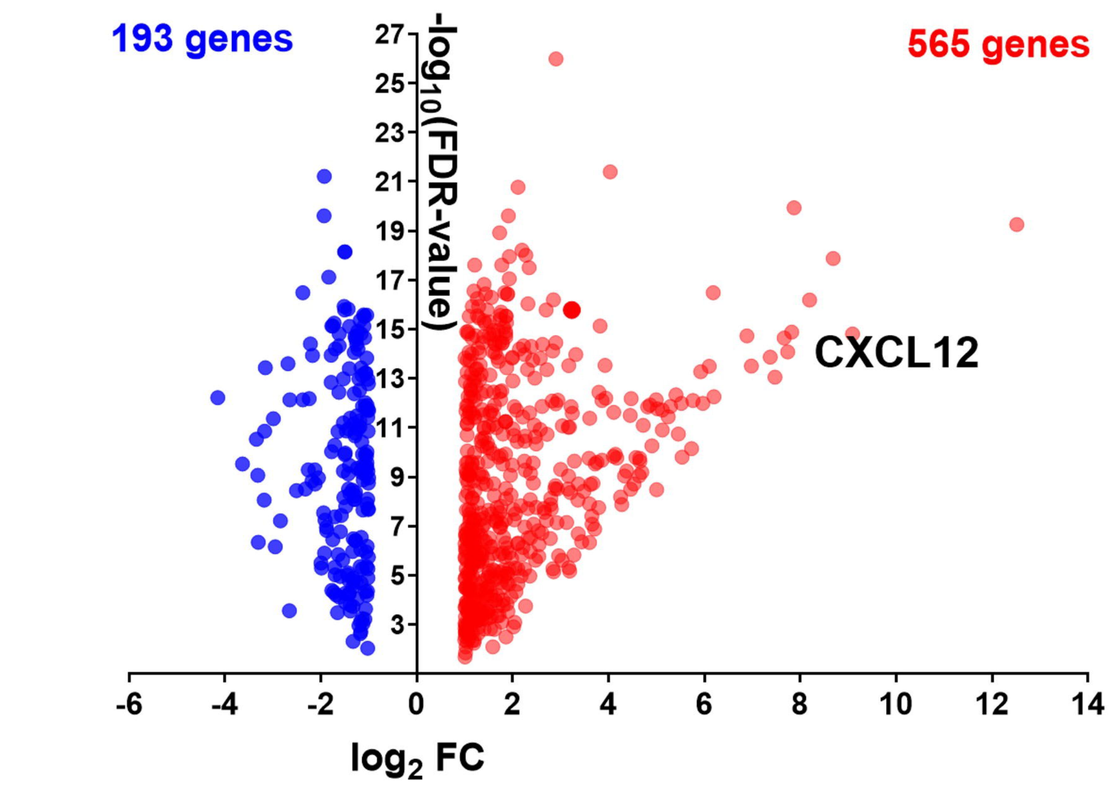
Mock-infected VERO-ZAP-WT vs. VERO-ZAP-KO, 24h
193 genes
565 genes
CXCL12
-log10(FDR-value)
log2 FC

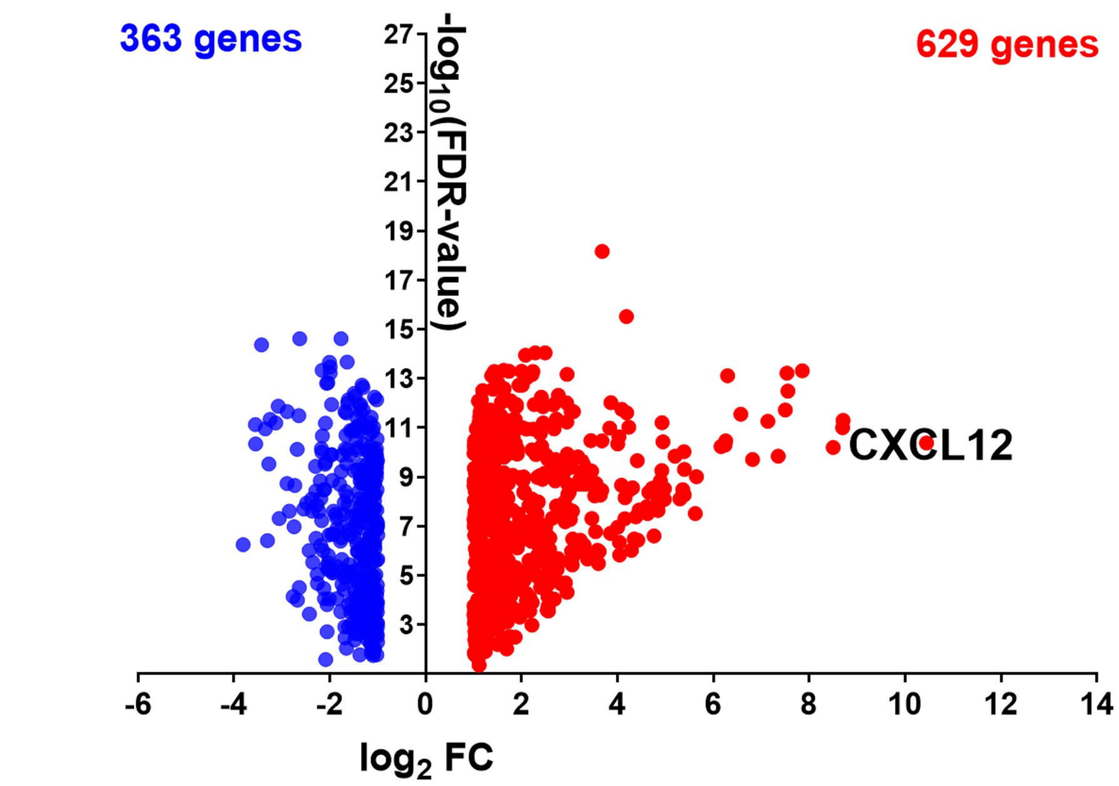
Mock-infected VERO-ZAP-WT vs. VERO-ZAP-KO, 72h
363 genes
629 genes
CXCL12
-log10(FDR-value)
log2 FC

B

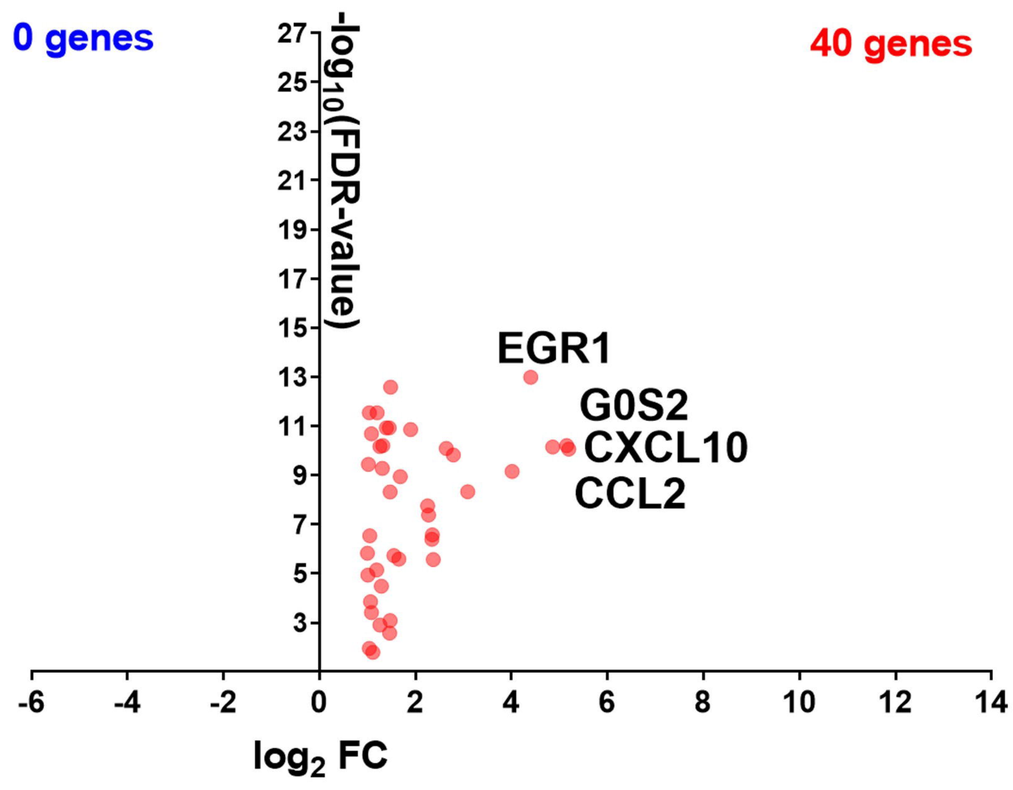
Mock-infected vs. Zika-infected VERO-ZAP-WT, 24h
0 genes
40 genes
EGR1
G0S2
CXCL10
CCL2
-log10(FDR-value)
log2 FC

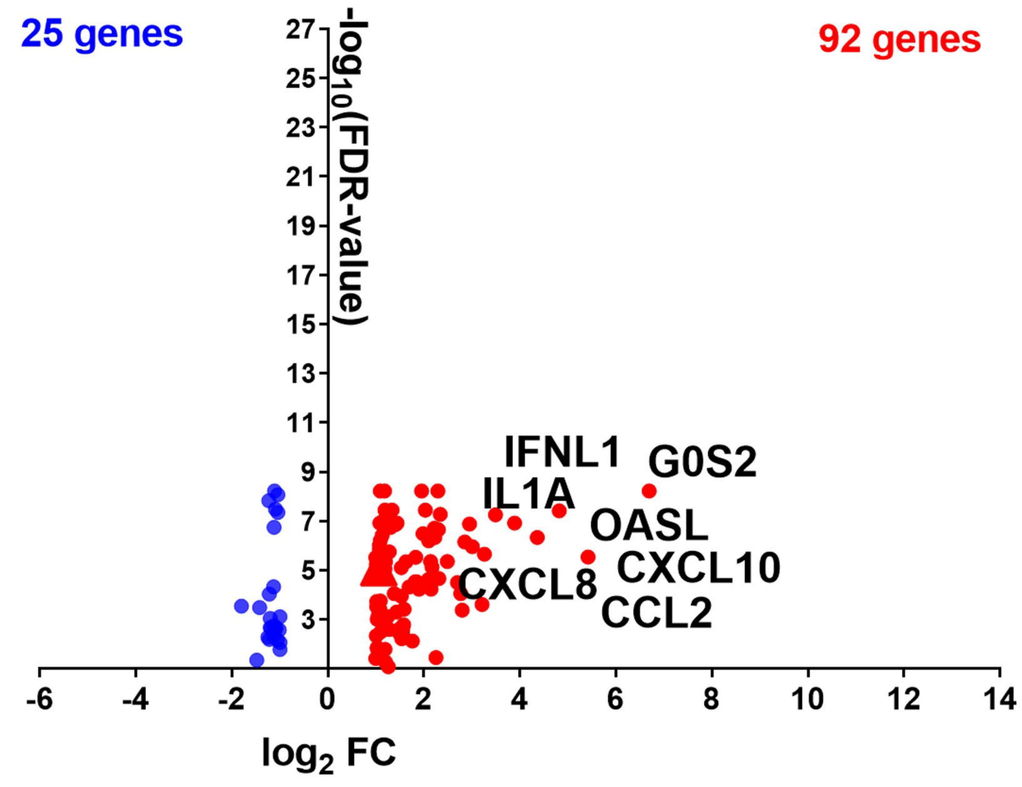
Mock-infected vs. Zika-infected VERO-ZAP-WT, 72h
25 genes
92 genes
IFNL1
G0S2
IL1A
OASL
CXCL10
CXCL8
CCL2
-log10(FDR-value)
log2 FC

C

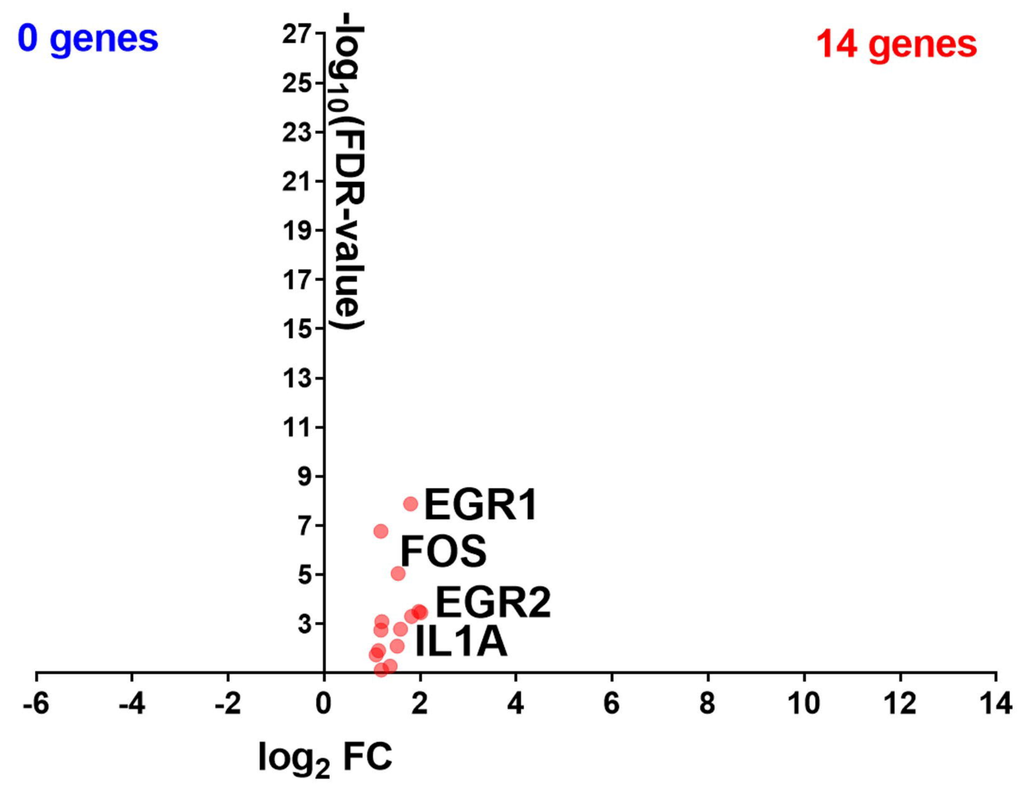
Mock-infected vs. Zika-infected VERO-ZAP-KO, 24h
0 genes
14 genes
EGR1
FOS
EGR2
IL1A
-log10(FDR-value)
log2 FC

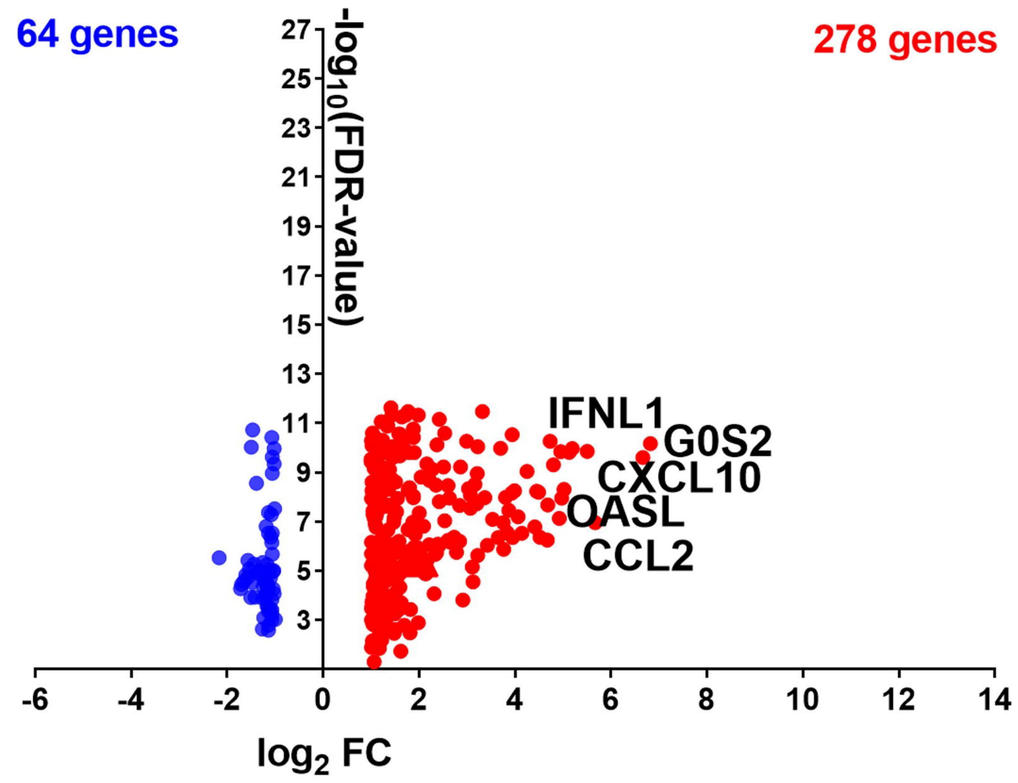
Mock-infected vs. Zika-infected VERO-ZAP-KO, 72h
64 genes
278 genes
IFNL1
G0S2
CXCL10
OASL
CCL2
-log10(FDR-value)
log2 FC

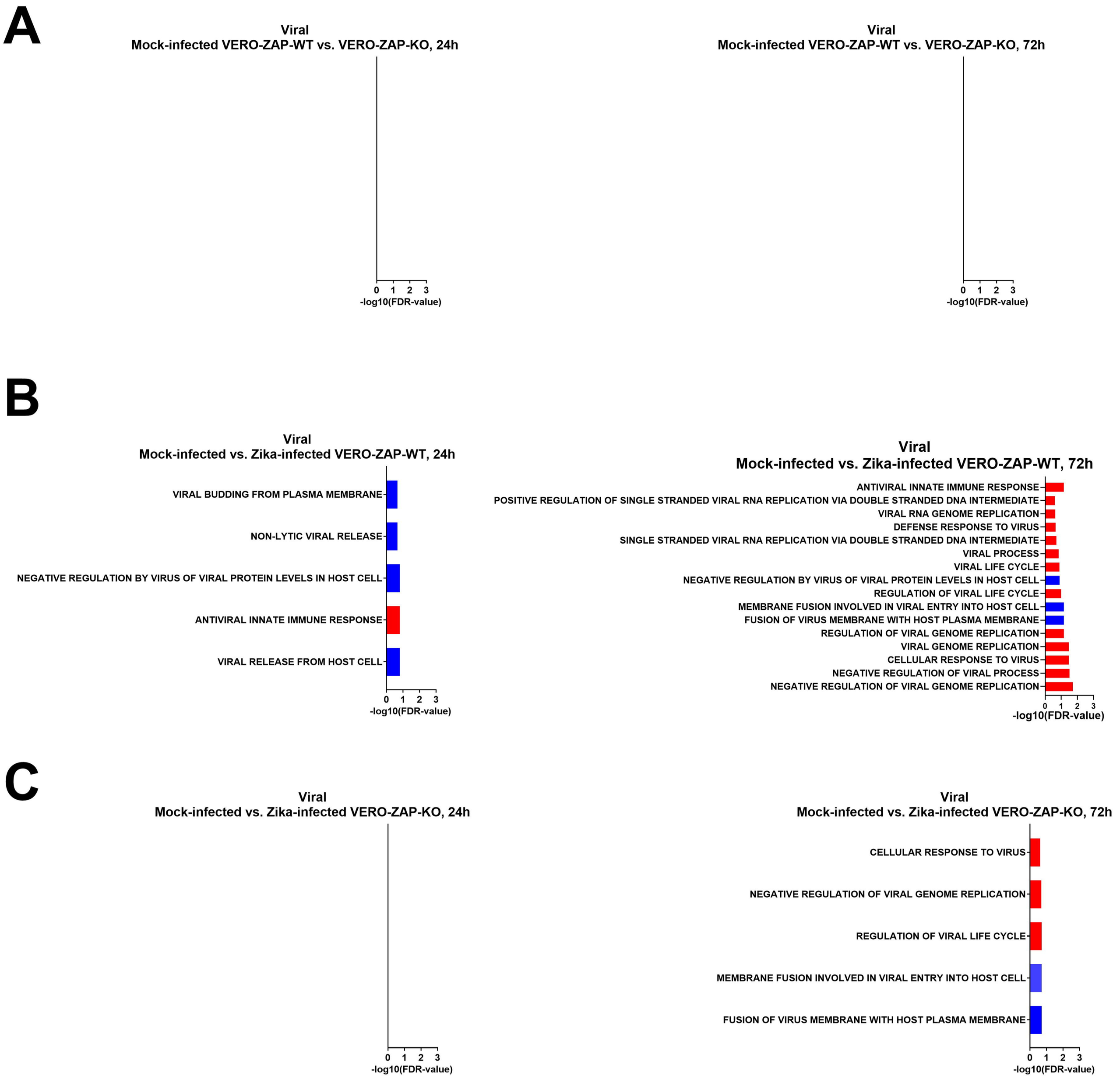
A
Viral
Mock-infected VERO-ZAP-WT vs. VERO-ZAP-KO, 24h
0 1 2 3
-log10(FDR-value)
Viral
Mock-infected VERO-ZAP-WT vs. VERO-ZAP-KO, 72h
0 1 2 3
-log10(FDR-value)
B
Viral
Mock-infected vs. Zika-infected VERO-ZAP-WT, 24h
VIRAL BUDDING FROM PLASMA MEMBRANE
NON-LYTIC VIRAL RELEASE
NEGATIVE REGULATION BY VIRUS OF VIRAL PROTEIN LEVELS IN HOST CELL
ANTIVIRAL INNATE IMMUNE RESPONSE
VIRAL RELEASE FROM HOST CELL
0 1 2 3
-log10(FDR-value)
Viral
Mock-infected vs. Zika-infected VERO-ZAP-WT, 72h
ANTIVIRAL INNATE IMMUNE RESPONSE
POSITIVE REGULATION OF SINGLE STRANDED VIRAL RNA REPLICATION VIA DOUBLE STRANDED DNA INTERMEDIATE
VIRAL RNA GENOME REPLICATION
DEFENSE RESPONSE TO VIRUS
SINGLE STRANDED VIRAL RNA REPLICATION VIA DOUBLE STRANDED DNA INTERMEDIATE
VIRAL PROCESS
VIRAL LIFE CYCLE
NEGATIVE REGULATION BY VIRUS OF VIRAL PROTEIN LEVELS IN HOST CELL
REGULATION OF VIRAL LIFE CYCLE
MEMBRANE FUSION INVOLVED IN VIRAL ENTRY INTO HOST CELL
FUSION OF VIRUS MEMBRANE WITH HOST PLASMA MEMBRANE
REGULATION OF VIRAL GENOME REPLICATION
VIRAL GENOME REPLICATION
CELLULAR RESPONSE TO VIRUS
NEGATIVE REGULATION OF VIRAL PROCESS
NEGATIVE REGULATION OF VIRAL GENOME REPLICATION
0 1 2 3
-log10(FDR-value)
C
Viral
Mock-infected vs. Zika-infected VERO-ZAP-KO, 24h
0 1 2 3
-log10(FDR-value)
Viral
Mock-infected vs. Zika-infected VERO-ZAP-KO, 72h
CELLULAR RESPONSE TO VIRUS
NEGATIVE REGULATION OF VIRAL GENOME REPLICATION
REGULATION OF VIRAL LIFE CYCLE
MEMBRANE FUSION INVOLVED IN VIRAL ENTRY INTO HOST CELL
FUSION OF VIRUS MEMBRANE WITH HOST PLASMA MEMBRANE
0 1 2 3
-log10(FDR-value)

A

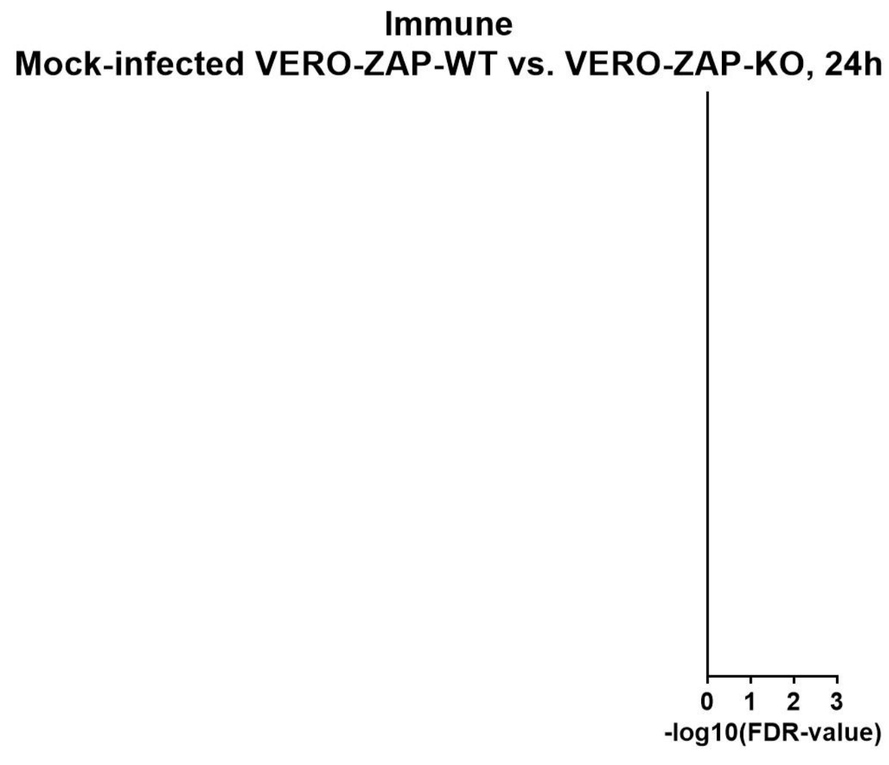
Immune
Mock-infected VERO-ZAP-WT vs. VERO-ZAP-KO, 24h
0 1 2 3
-log10(FDR-value)

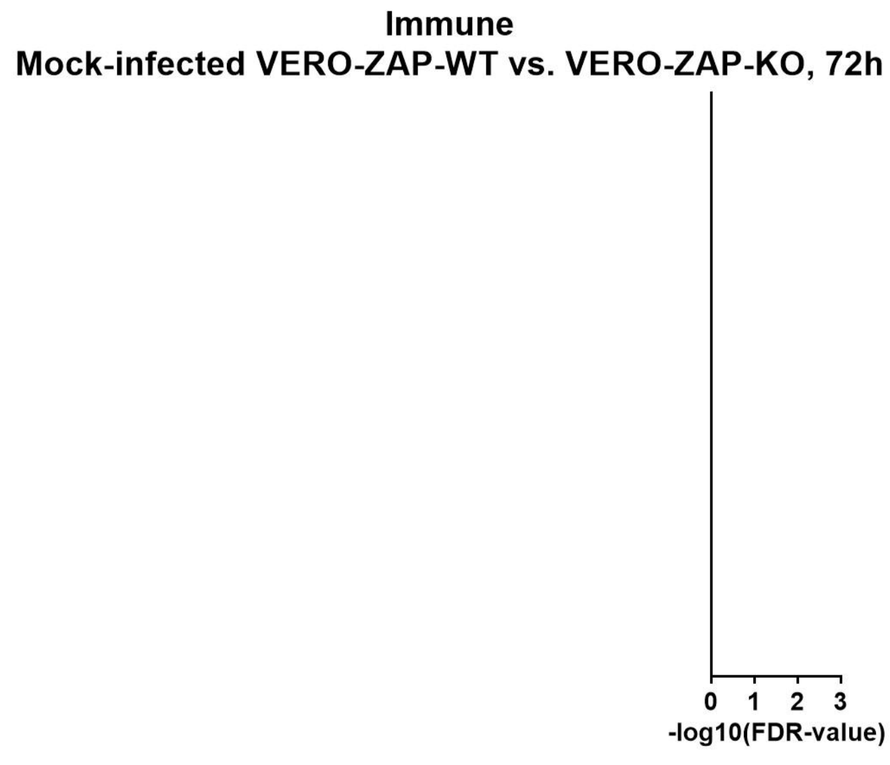
Immune
Mock-infected VERO-ZAP-WT vs. VERO-ZAP-KO, 72h
0 1 2 3
-log10(FDR-value)

B

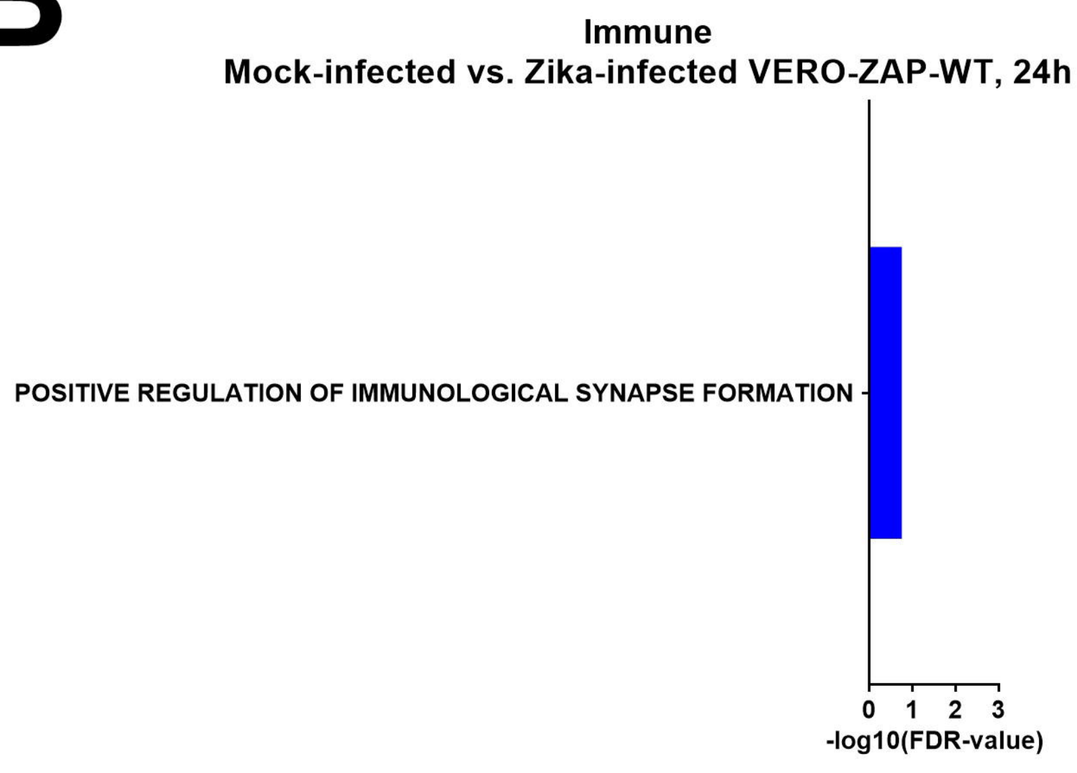
Immune
Mock-infected vs. Zika-infected VERO-ZAP-WT, 24h
POSITIVE REGULATION OF IMMUNOLOGICAL SYNAPSE FORMATION
0 1 2 3
-log10(FDR-value)

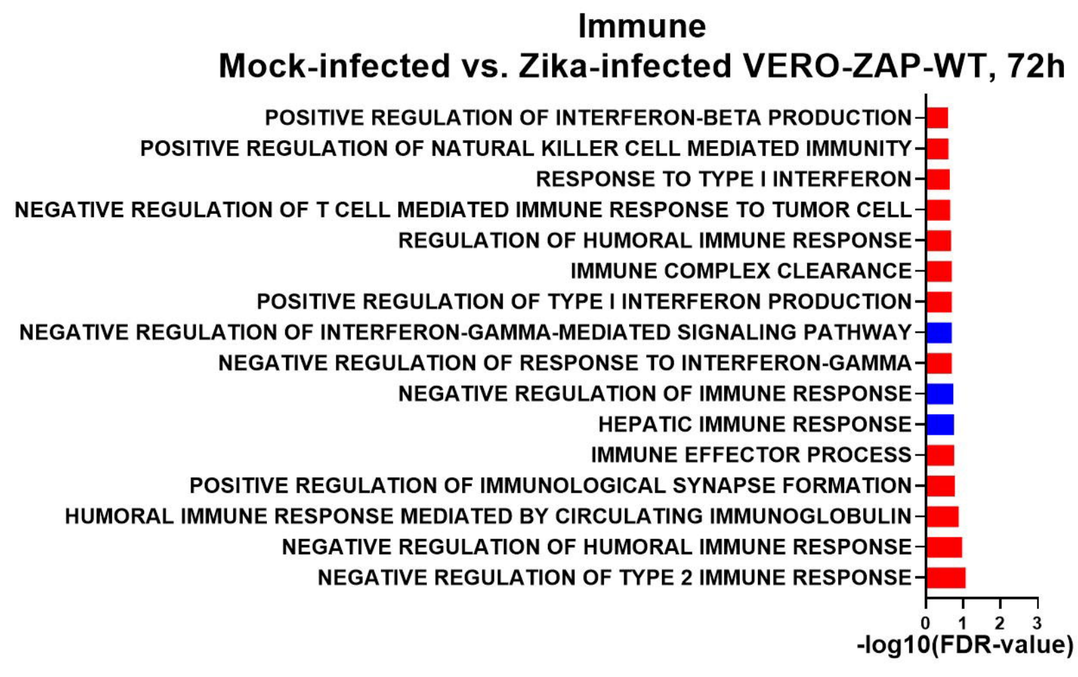
Immune
Mock-infected vs. Zika-infected VERO-ZAP-WT, 72h
POSITIVE REGULATION OF INTERFERON-BETA PRODUCTION
POSITIVE REGULATION OF NATURAL KILLER CELL MEDIATED IMMUNITY
RESPONSE TO TYPE I INTERFERON
NEGATIVE REGULATION OF T CELL MEDIATED IMMUNE RESPONSE TO TUMOR CELL
REGULATION OF HUMORAL IMMUNE RESPONSE
IMMUNE COMPLEX CLEARANCE
POSITIVE REGULATION OF TYPE I INTERFERON PRODUCTION
NEGATIVE REGULATION OF INTERFERON-GAMMA-MEDIATED SIGNALING PATHWAY
NEGATIVE REGULATION OF RESPONSE TO INTERFERON-GAMMA
NEGATIVE REGULATION OF IMMUNE RESPONSE
HEPATIC IMMUNE RESPONSE
IMMUNE EFFECTOR PROCESS
POSITIVE REGULATION OF IMMUNOLOGICAL SYNAPSE FORMATION
HUMORAL IMMUNE RESPONSE MEDIATED BY CIRCULATING IMMUNOGLOBULIN
NEGATIVE REGULATION OF HUMORAL IMMUNE RESPONSE
NEGATIVE REGULATION OF TYPE 2 IMMUNE RESPONSE
0 1 2 3
-log10(FDR-value)

C

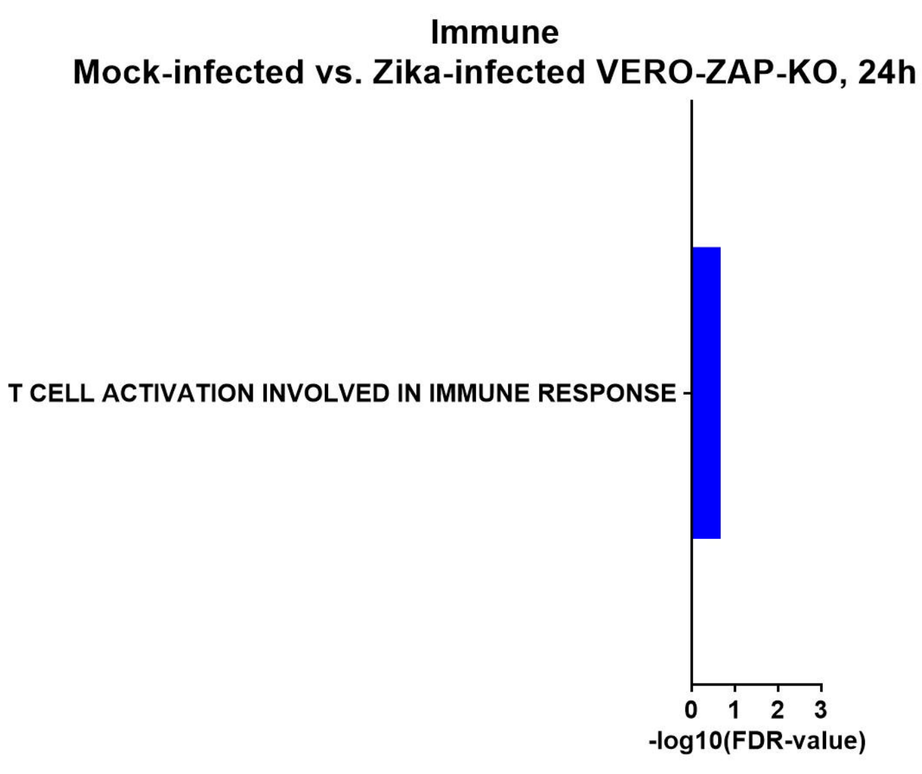
Immune
Mock-infected vs. Zika-infected VERO-ZAP-KO, 24h
T CELL ACTIVATION INVOLVED IN IMMUNE RESPONSE
0 1 2 3
-log10(FDR-value)

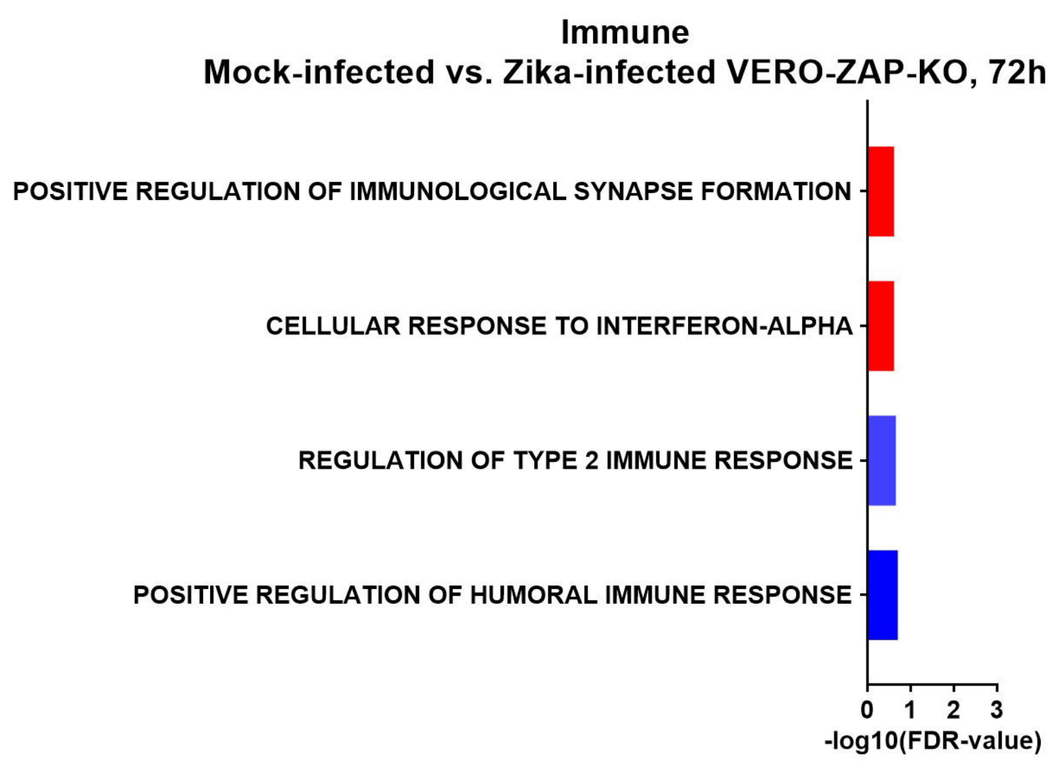
Immune
Mock-infected vs. Zika-infected VERO-ZAP-KO, 72h
POSITIVE REGULATION OF IMMUNOLOGICAL SYNAPSE FORMATION
CELLULAR RESPONSE TO INTERFERON-ALPHA
REGULATION OF TYPE 2 IMMUNE RESPONSE
POSITIVE REGULATION OF HUMORAL IMMUNE RESPONSE
0 1 2 3
-log10(FDR-value)

A

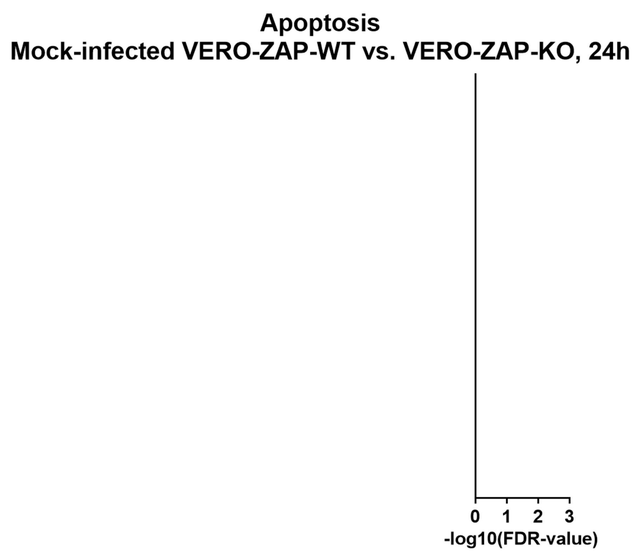
Apoptosis
Mock-infected VERO-ZAP-WT vs. VERO-ZAP-KO, 24h
0 1 2 3
-log10(FDR-value)

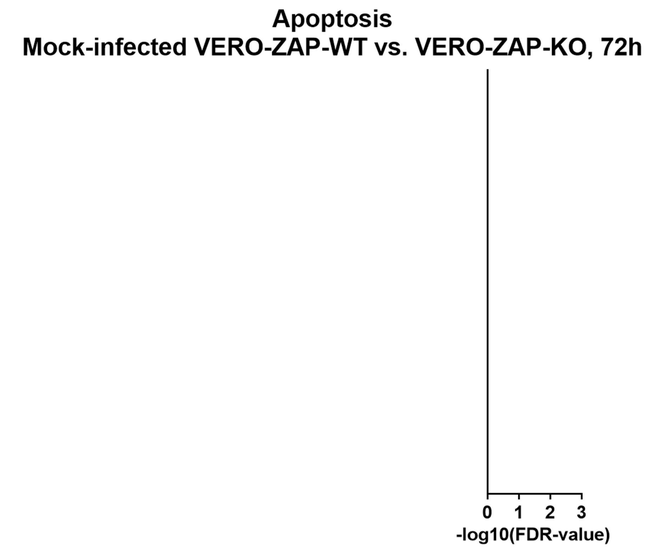
Apoptosis
Mock-infected VERO-ZAP-WT vs. VERO-ZAP-KO, 72h
0 1 2 3
-log10(FDR-value)

B

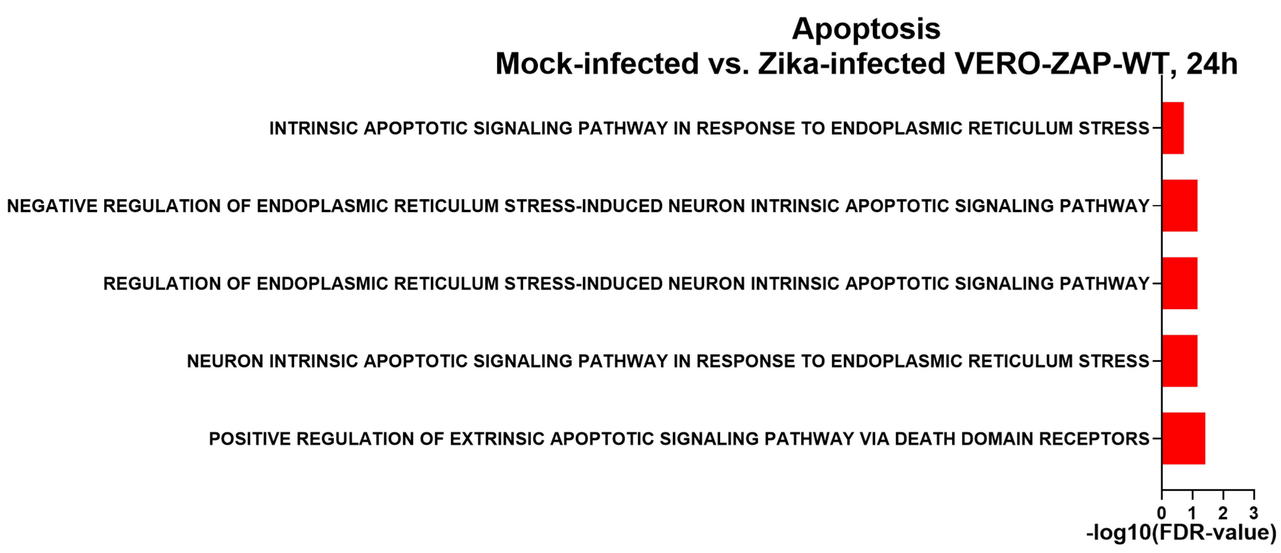
Apoptosis
Mock-infected vs. Zika-infected VERO-ZAP-WT, 24h
INTRINSIC APOPTOTIC SIGNALING PATHWAY IN RESPONSE TO ENDOPLASMIC RETICULUM STRESS
NEGATIVE REGULATION OF ENDOPLASMIC RETICULUM STRESS-INDUCED NEURON INTRINSIC APOPTOTIC SIGNALING PATHWAY
REGULATION OF ENDOPLASMIC RETICULUM STRESS-INDUCED NEURON INTRINSIC APOPTOTIC SIGNALING PATHWAY
NEURON INTRINSIC APOPTOTIC SIGNALING PATHWAY IN RESPONSE TO ENDOPLASMIC RETICULUM STRESS
POSITIVE REGULATION OF EXTRINSIC APOPTOTIC SIGNALING PATHWAY VIA DEATH DOMAIN RECEPTORS
0 1 2 3
-log10(FDR-value)

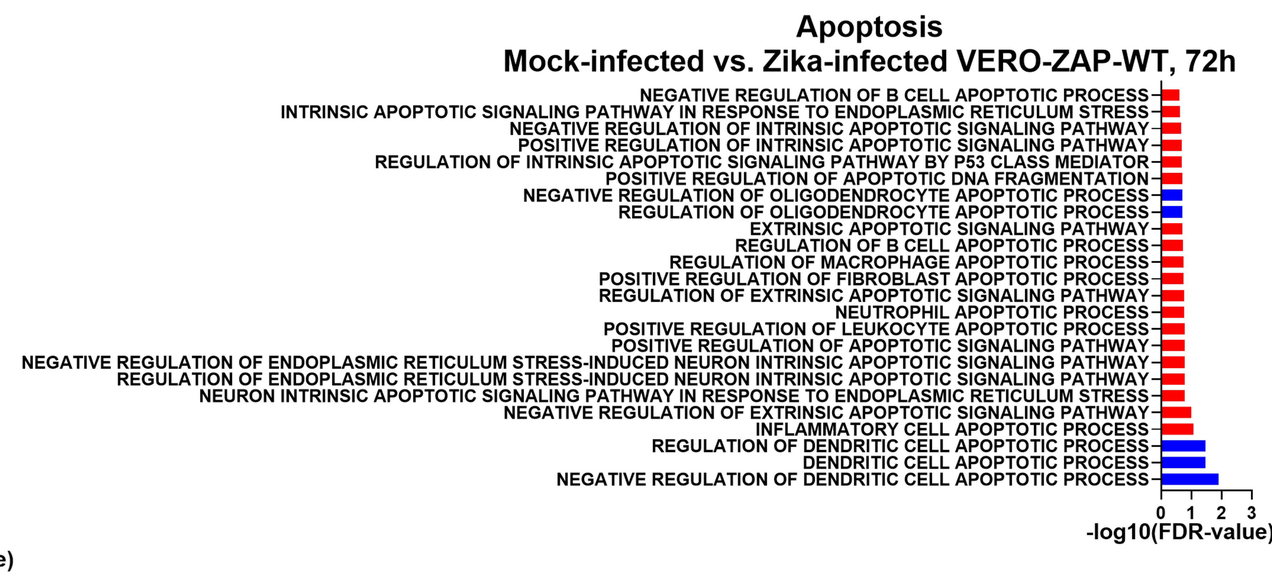
Apoptosis
Mock-infected vs. Zika-infected VERO-ZAP-WT, 72h
NEGATIVE REGULATION OF B CELL APOPTOTIC PROCESS
INTRINSIC APOPTOTIC SIGNALING PATHWAY IN RESPONSE TO ENDOPLASMIC RETICULUM STRESS
NEGATIVE REGULATION OF INTRINSIC APOPTOTIC SIGNALING PATHWAY
POSITIVE REGULATION OF INTRINSIC APOPTOTIC SIGNALING PATHWAY
REGULATION OF INTRINSIC APOPTOTIC SIGNALING PATHWAY BY P53 CLASS MEDIATOR
POSITIVE REGULATION OF APOPTOTIC DNA FRAGMENTATION
NEGATIVE REGULATION OF OLIGODENDROCYTE APOPTOTIC PROCESS
REGULATION OF OLIGODENDROCYTE APOPTOTIC PROCESS
EXTRINSIC APOPTOTIC SIGNALING PATHWAY
REGULATION OF B CELL APOPTOTIC PROCESS
REGULATION OF MACROPHAGE APOPTOTIC PROCESS
POSITIVE REGULATION OF FIBROBLAST APOPTOTIC PROCESS
REGULATION OF EXTRINSIC APOPTOTIC SIGNALING PATHWAY
NEUTROPHIL APOPTOTIC PROCESS
POSITIVE REGULATION OF LEUKOCYTE APOPTOTIC PROCESS
POSITIVE REGULATION OF APOPTOTIC SIGNALING PATHWAY
NEGATIVE REGULATION OF ENDOPLASMIC RETICULUM STRESS-INDUCED NEURON INTRINSIC APOPTOTIC SIGNALING PATHWAY
REGULATION OF ENDOPLASMIC RETICULUM STRESS-INDUCED NEURON INTRINSIC APOPTOTIC SIGNALING PATHWAY
NEURON INTRINSIC APOPTOTIC SIGNALING PATHWAY IN RESPONSE TO ENDOPLASMIC RETICULUM STRESS
NEGATIVE REGULATION OF EXTRINSIC APOPTOTIC SIGNALING PATHWAY
INFLAMMATORY CELL APOPTOTIC PROCESS
REGULATION OF DENDRITIC CELL APOPTOTIC PROCESS
DENDRITIC CELL APOPTOTIC PROCESS
NEGATIVE REGULATION OF DENDRITIC CELL APOPTOTIC PROCESS
0 1 2 3
-log10(FDR-value)

C

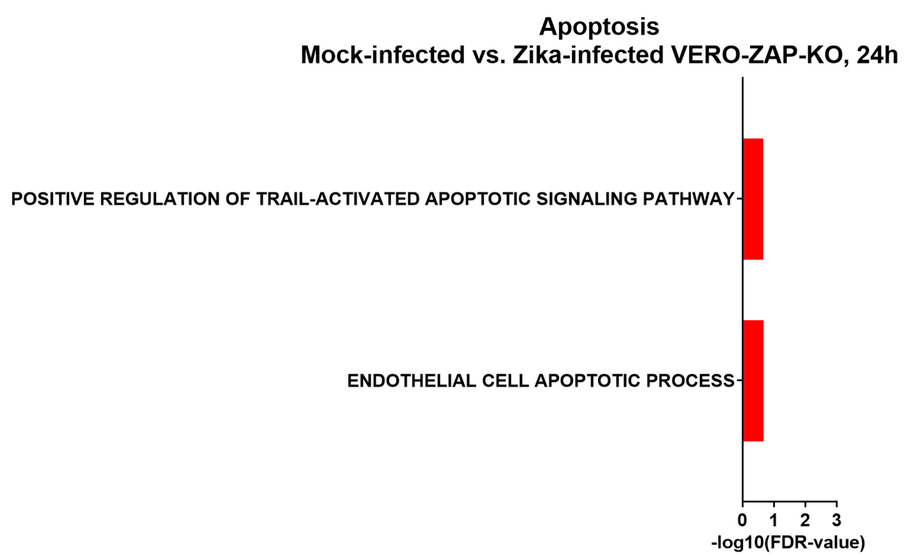
Apoptosis
Mock-infected vs. Zika-infected VERO-ZAP-KO, 24h
POSITIVE REGULATION OF TRAIL-ACTIVATED APOPTOTIC SIGNALING PATHWAY
ENDOTHELIAL CELL APOPTOTIC PROCESS
0 1 2 3
-log10(FDR-value)

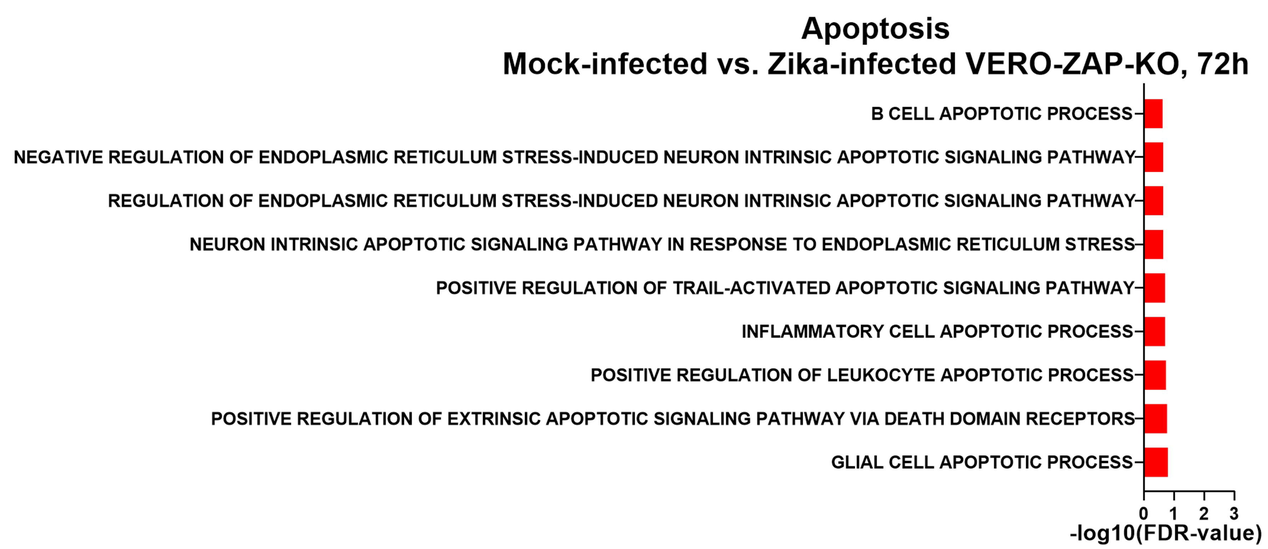
Apoptosis
Mock-infected vs. Zika-infected VERO-ZAP-KO, 72h
B CELL APOPTOTIC PROCESS
NEGATIVE REGULATION OF ENDOPLASMIC RETICULUM STRESS-INDUCED NEURON INTRINSIC APOPTOTIC SIGNALING PATHWAY
REGULATION OF ENDOPLASMIC RETICULUM STRESS-INDUCED NEURON INTRINSIC APOPTOTIC SIGNALING PATHWAY
NEURON INTRINSIC APOPTOTIC SIGNALING PATHWAY IN RESPONSE TO ENDOPLASMIC RETICULUM STRESS
POSITIVE REGULATION OF TRAIL-ACTIVATED APOPTOTIC SIGNALING PATHWAY
INFLAMMATORY CELL APOPTOTIC PROCESS
POSITIVE REGULATION OF LEUKOCYTE APOPTOTIC PROCESS
POSITIVE REGULATION OF EXTRINSIC APOPTOTIC SIGNALING PATHWAY VIA DEATH DOMAIN RECEPTORS
GLIAL CELL APOPTOTIC PROCESS
0 1 2 3
-log10(FDR-value)

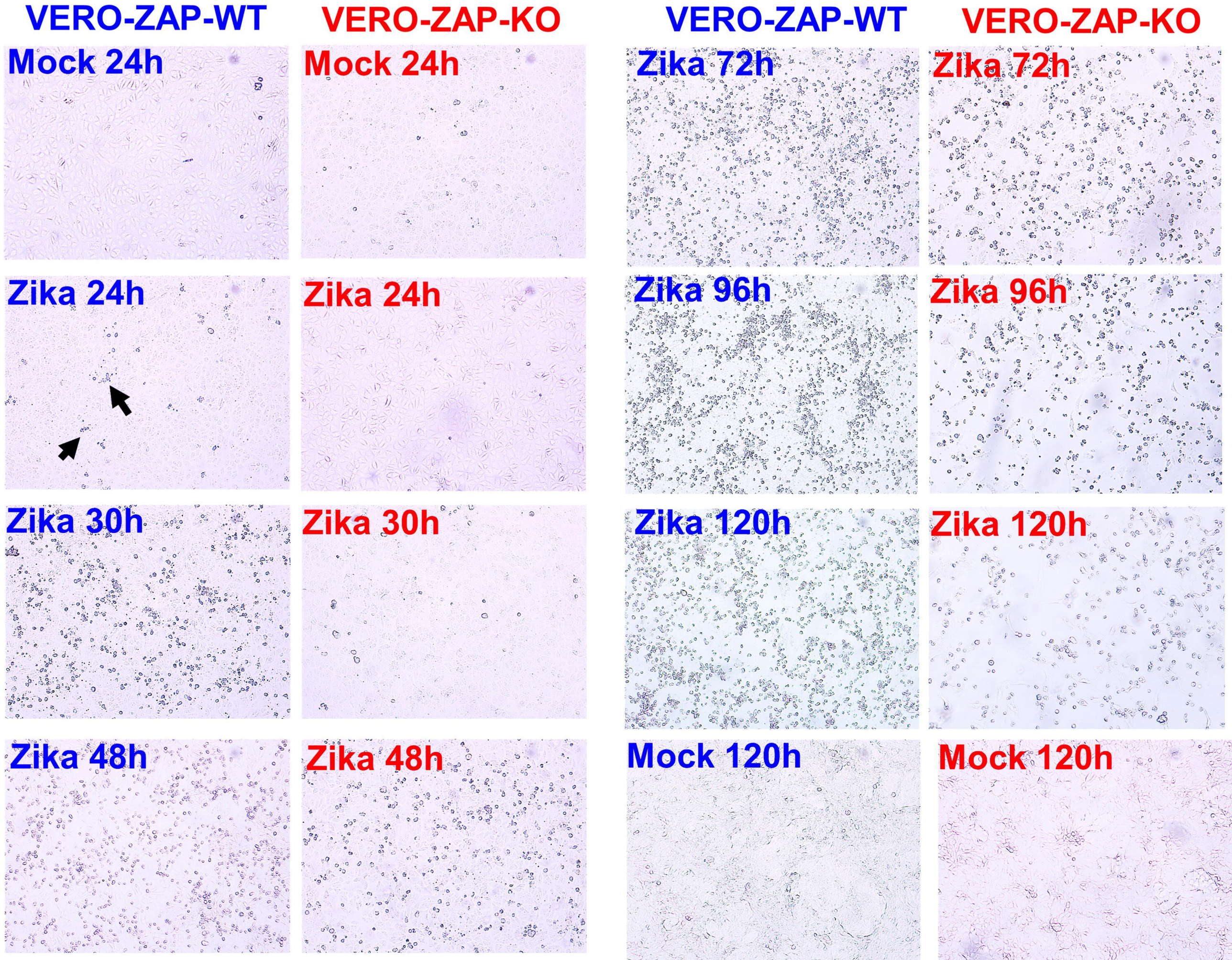
VERO-ZAP-WT
VERO-ZAP-KO
VERO-ZAP-WT
VERO-ZAP-KO
Mock 24h
Mock 24h
Zika 72h
Zika 72h
Zika 24h
Zika 24h
Zika 96h
Zika 96h
Zika 30h
Zika 30h
Zika 120h
Zika 120h
Zika 48h
Zika 48h
Mock 120h
Mock 120h